PART II

ALIPHATIC POLYESTER BLENDS

CHAPTER 7

Stereocomplexation Between Enantiomeric Poly(lactide)s

HIDETO TSUJI

Department of Ecological Engineering, Faculty of Engineering, Toyohashi University of Technology, Aichi, Japan

YOSHITO IKADA

Department of Environmental Medicine, Faculty of Medicine, Nara Medical University, Nara, Japan

7.1 INTRODUCTION

Poly(lactide) or poly(lactic acid) (PLA) is producible from renewable resources such as starch, is biodegradable in the human body as well as in the environment, is compostable, and is not toxic to the human body and the environment (Coombes and Meikle, 1994; Doi and Fukuda, 1994; Kharas et al., 1994; Vert et al., 1995; Hartmann, 1998; Ikada and Tsuji, 2000; Garlotta, 2001; Albertsson, 2002; Scott,

Biodegradable Polymer Blends and Composites from Renewable Resources. Edited by Long Yu

2002; Södergård and Stolt, 2002; Tsuji, 2002a, 2007; Auras et al., 2004; Yu et al., 2006; Gupta et al., 2007). Because of these properties, PLA has been studied intensively for more than forty years in terms of scientific and industrial interest. The synthesis, recycling, and biodegradation of PLA are schematically represented in Fig. 7-1 (Tsuji, 2007). PLA has high mechanical performance similar to that of representative commercial polymers such as polyethylene and poly(ethylene terephthalate) (PET).

PLA-based materials have been used for biomedical, pharmaceutical, environmental, industrial, and commodity applications. Because of good biodegradability and very low toxicity, PLA and lactide (LA) copolymers have been used as biomedical material for fixation of fractured bone and as matrices for drug delivery systems. Poly(L-lactide) composite materials are also used in automobile parts and the casings for personal computers and mobile phones. The physical properties and biodegradation behavior of PLA can be modified depending on their applications. Manipulation of the physical characteristics and biodegradation kinetics will employ blending and composite formation by selection of the filler (second polymer) type and concentration, for reasons of simplicity and commercial advantage. From among the PLA-based polymer blends, this chapter focuses on blends of poly(L-lactide) (PLLA) with poly(D-lactide) (PDLA), as stereocomplex formation takes place upon blending of PLLA with PDLA. Since this stereocomplexation between enantiomeric PLAs (i.e., PLLA and PDLA) was first reported by us (Ikada et al., 1987), numerous studies have addressed the formation, structure, physical properties, degradation, and applications of the PLA stereocomplex (Slager and Domb et al., 2003a; Tsuji, 2005). Stereocomplexation enhances mechanical properties, thermal resistance, and hydrolytic degradation resistance of PLA-based materials. These improvements arise

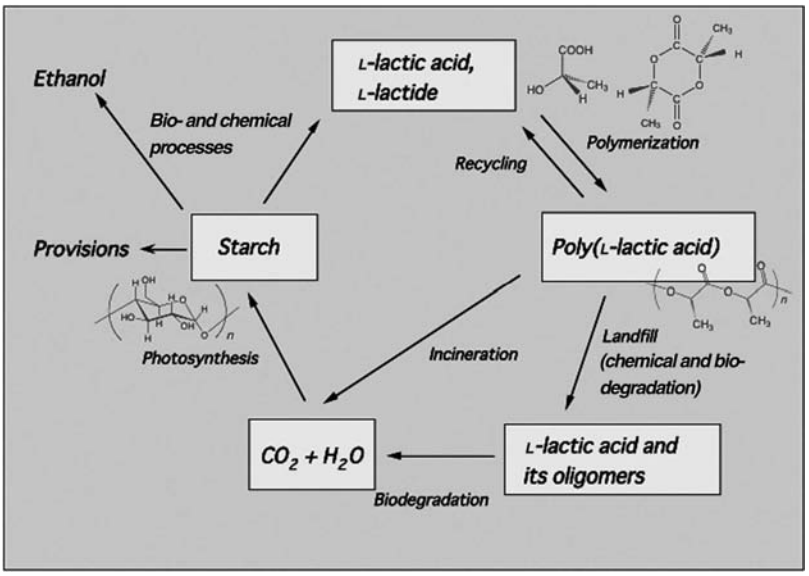

Fig. 7-1 Synthesis, recycling, and degradation of poly(L-lactide) (PLLA) (Tsuji, 2007).

from a strong interaction between L-lactyl and D-lactyl unit sequences, opening a new route for preparation of novel hydrogels and particles for biomedical applications. It has been shown that crucial parameters affecting the stereocomplexation include the mixing ratio and molecular weights of L-lactyl and D-lactyl unit sequences. The polymer pairs and stereoblock copolymers that may give rise to complexation are summarized in review articles (Slager and Domb, 2003a; Tsuji, 2005).

7.2 STEREOCOMPLEX FORMATION

The synthetic routes for LA or lactic acid homopolymers having a variety of tacticity and optical purity are summarized in Fig. 7-2 (Tsuji, 2005). The unit cell parameters of pure PLLA and PLA stereocomplex are summarized in Table 7-1 (2002a). Nonblended PLLA has been reported to crystallize in three forms: α-form (De Santis and Kovacs, 1968; Hoogsteen et al., 1990; Kobayashi et al., 1995), β-form (Hoogsteen et al., 1990; Puiggali et al., 2000), and γ-form (Cartier et al., 2000). The β-form of pure PLLA has a rather frustrated structure (Puiggali et al., 2000), but the stereocomplex crystal has a triclinic unit cell, in which PLLA and PDLA chains taking a 3_1 helical conformation are packed side-by-side in a parallel fashion. PLLA can crystallize in the temperature range 75–160°C and the radius growth rate of spherulite (G) shows the maximum at 130°C (Kalb and Pennings, 1981; Tsuji and Ikada, 1995; Abe et al., 2001; Di Lorenzo, 2005; Tsuji et al., 2005a, b). The crystallization mechanism changes from Regime III to Regime II at 120°C and Regime II to Regime I at 163°C (Kalb and Pennings, 1980; Abe et al., 2001; Di Lorenzo, 2005; Tsuji et al., 2005a, b). It has been suggested that the presence of two G maxima or the regime change from III to II is associated with the crystalline, structural change from α′-form to α-form at 110–130°C (Zhang et al., 2005a; Kawai et al., 2007; Pan et al., 2008).

On the other hand, as seen in Fig. 7-3, main peaks of PDLA ($X_D = 1$) film appear at 2θ values of 15°, 17°, and 19° (Ikada et al., 1987), which are comparable to those for the α-form of PLLA crystallized in a pseudo-orthorhombic unit cell with two 10_3 helices and the dimensions $a = 1.07$ nm, $b = 0.595$ nm, and $c = 2.78$ nm (Okihara et al., 1991). The most intense peaks of equimolar blended film ($X_D = 0.5$) are observed at 2θ values of 12°, 21°, and 24°, where X_D is defined as

$$X_D = \frac{\text{weight of PDLA}}{\text{weight of PLLA and PDLA}} \tag{7.1}$$

They correspond to those of the PLA stereocomplex crystallized in a triclinic unit cell of dimensions $a = 0.916$ nm, $b = 0.916$ nm, $c = 0.870$ nm, $\alpha = 109.2°$, $\beta = 109.2°$, and $\gamma = 109.8°$, in which L-lactide (LLA) and D-lactide (DLA) segments are packed parallel taking a 3_1 helical conformation (Okihara et al., 1991). The crystal structure of the PLA stereocomplex is demonstrated in Fig. 7-4. The lattice containing one PLLA or PDLA chain with a 3_1 helical conformation has the shape of an equilateral

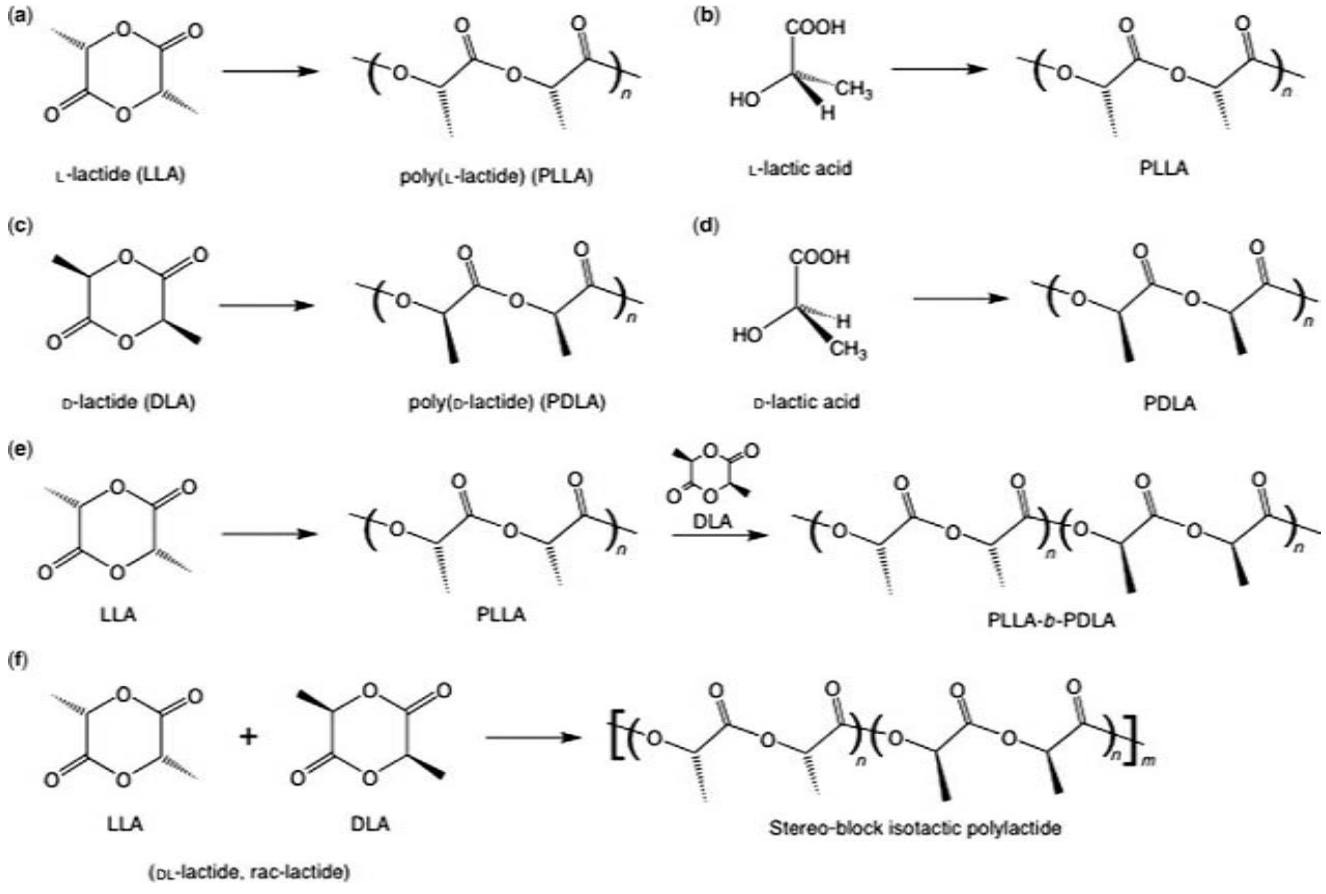

Fig. 7-2 Synthesis and molecular structures of PLLA (a and b), PDLA (c and d), and stereoblock isotactic PLA (e and f) (Tsuji, 2005).

TABLE 7-1 Unit Cell Parameters Reported for Non-Blended PLLA and Stereocomplex Crystals [Tsuji, 2002a]

	Space Group	Chain Orientation	Number of Helices Per Unit Cell	Helical Conformation	a (nm)	b (nm)	c (nm)	α (deg.)	β (deg.)	γ (deg.)
PLLA (α-form) (De Santis and Kovacs, 1968)	Pseudo-orthorhombic	–	2	10_3	1.07	0.645	2.78	90	90	90
PLLA (α-form) (Hoogsteen et al., 1990)	Pseudo-orthorhombic	–	2	10_3	1.06	0.61	2.88	90	90	90
PLLA (α-form) (Kobayashi et al., 1995)	Orthorhombic	–	2	10_3	1.05	0.61	2.88	90	90	90
PLLA (β-form) (Hoogsteen et al., 1990)	Orthorhombic	–	6	3_1	1.031	1.821	0.90	90	90	90
PLLA (β-form) (Puiggali et al., 2000)	Trigonal	Random up-down	3	3_1	1.052	1.052	0.88	90	90	120
PLLA (γ-form) (Cartier et al., 2000)	Orthorhombic	Antiparallel	2	3_1	0.995	0.625	0.88	90	90	90
Stereocomplex (Okihara et al., 1991)	Triclinic	Parallel	2	3_1	0.916	0.916	0.870	109.2	109.2	109.8

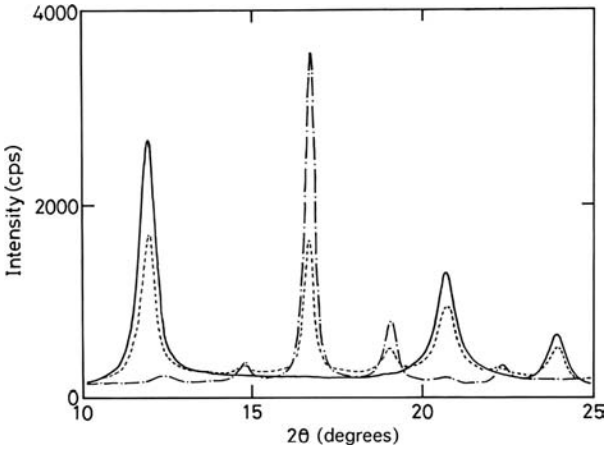

Fig. 7-3 WAXS profiles of PLLA/PDLA blends having different X_D values (Ikada et al., 1987). Solid line, dashed line, and dashed/single dotted line are for $X_D = 0.5$, 0.75, and 1, respectively.

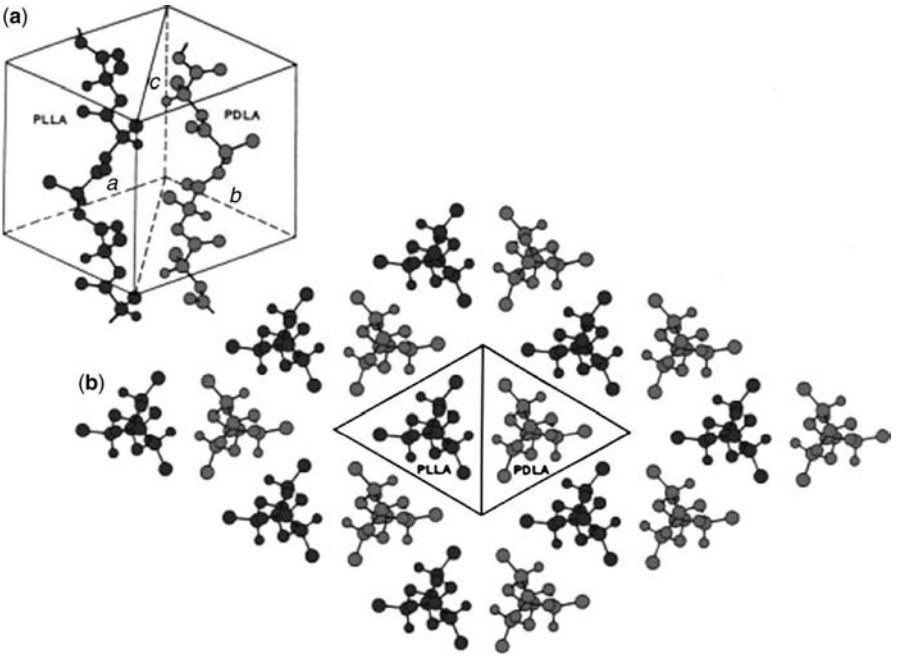

Fig. 7-4 Crystal structure of PLA stereocomplex (Okihara et al., 1991). The lines between PLLA and PDLA chains have been added to the original figure.

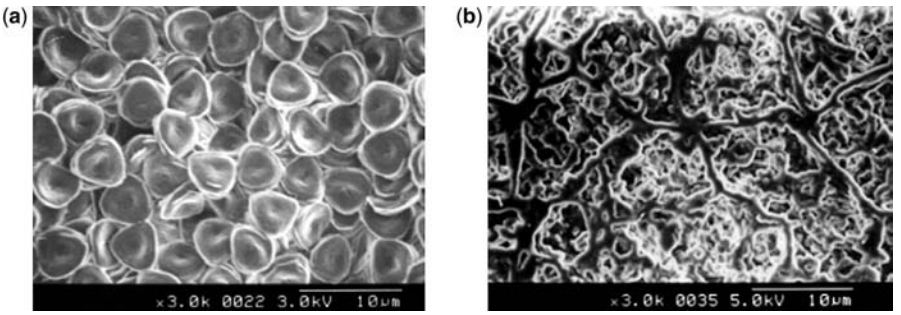

Fig. 7-5 PLA stereocomplex formed in dilute solution (single crystals) (a) (Tsuji et al., 1992) and concentrated solution (dried gel) (b) (Tsuji and Ikada, 1999).

triangle. This is expected to form equilateral-triangle-shaped single crystals of PLA stereocomplex. Equilateral-triangular single crystals [Okihara et al., 1991; Tsuji et al., 1992 (Fig. 7-5a); Brizzolara et al., 1996] and gels [Tsuji and Ikada, 1999 (Fig. 7-5b)] of PLA stereocomplex were formed when crystallized in a solution. Brizzolara et al. proposed the crystallization mechanism of PLA stereocomplex shown in Fig. 7-6 (Brizzolara et al., 1996).

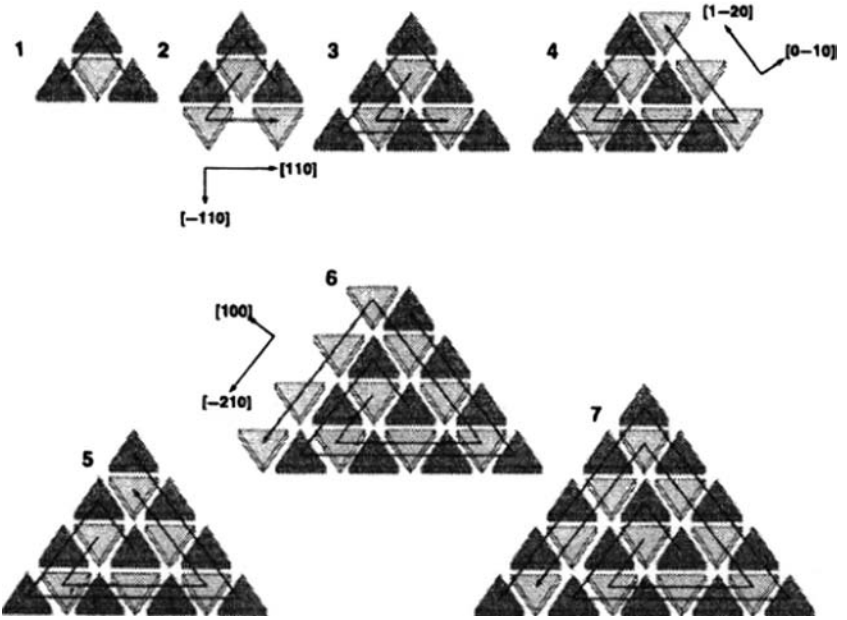

Fig. 7-6 Schematic growth mechanism of the stereocomplex single crystal (Brizzolara et al., 1996). Reprinted with permission from *Macromolecules*. Copyright (1996) American Chemical Society.

DSC and WAXS measurements of PLLA/PDLA blends having different X_D values first confirmed PLA stereocomplexation, as shown in Fig. 7-7 (Tsuji et al., 1991a) and Fig. 7-3 (Ikada et al., 1987), respectively. The specimens were prepared by precipitation of PLLA and PDLA in methylene chloride mixed solution with stirred methanol. The peak seen in Fig. 7-7 at 180°C for PLLA or PDLA ($X_D = 0$ or 1) is ascribed to the melting of PLLA or PDLA homocrystallites composed of either PLLA or PDLA chains alone. In contrast, a new melting peak appears at 230°C in the blend specimens, irrespective of X_D. The new peak is due to the melting of stereocomplex crystallites.

The difficulty of keeping PLLA/PDLA blends with molecular weights in the order of 10^3 g/mol in the amorphous state by melt-quenching strongly suggests that the overall crystallization rate of PLA stereocomplex is much higher than that of homocrystallites of PLLA or PDLA alone. This was evidenced by polarized optical microscopy (Tsuji and Tezuka, 2004), as represented in Fig. 7-8 for PLLA/PDLA blend and pure PLLA and PDLA films crystallized from their melt. Figure 7-9 shows G values of the spherulites of stereocomplex crystallites in PLLA/PDLA blends and homocrystallites in pure PLLA and PDLA films, and the

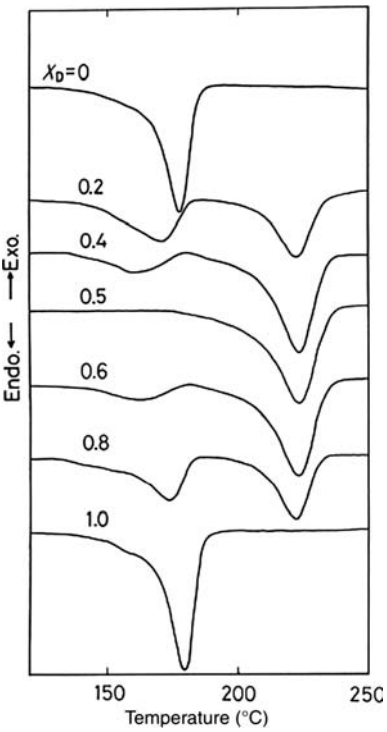

Fig. 7-7 DSC thermograms of PLLA/PDLA blends with different X_D values (Tsuji et al., 1991a). Viscosity-average molecular weight (M_v) of both PLLA and PLLA is 3.6×10^5 g/mol.

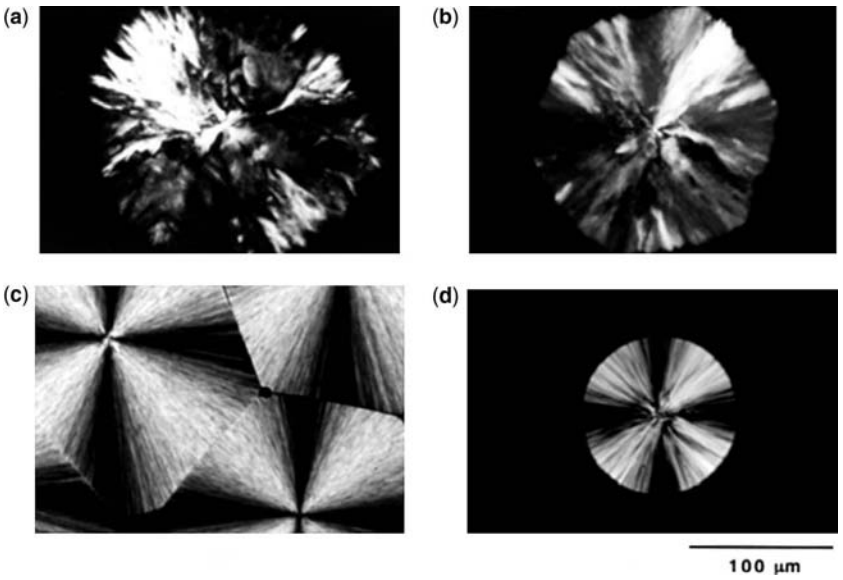

Fig. 7-8 Spherulites of PLLA ($X_D = 0$) ($M_w = 1.0 \times 10^4$ g/mol) (a), PDLA ($X_D = 1$) ($M_w = 2.2 \times 10^4$ g/mol) (b), and their blend ($X_D = 0.5$) (c, d) films crystallized at 140°C (a–c) and 190°C (d) from the melt at 250°C. Crystallization times were 11, 6, 0.5, and 12 min for (a), (b), (c), and (d), respectively (Tsuji and Tezuka, 2004).

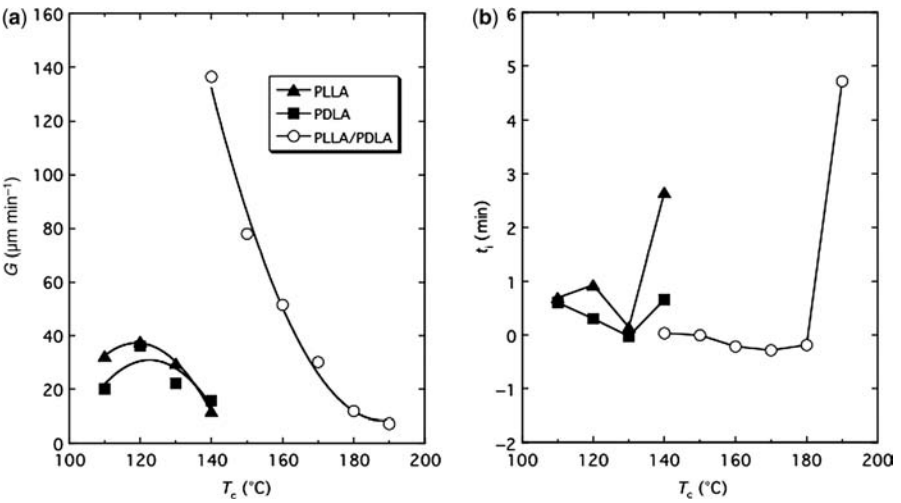

Fig. 7-9 Radius growth rate of spherulites (G) and induction period of spherulite formation (t_i) of PLLA ($X_D = 0$), PDLA ($X_D = 1$), and their blend ($X_D = 0.5$) films as functions of crystallization temperature (T_c) (Tsuji and Tezuka, 2004).

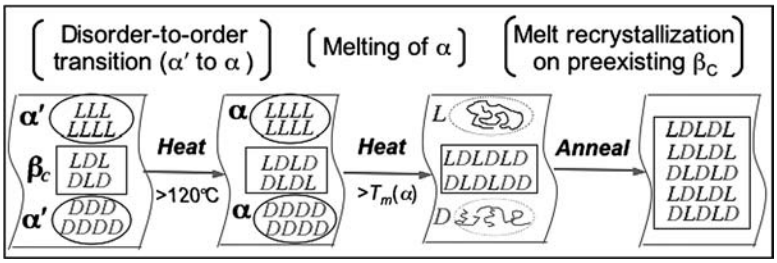

Fig. 7-10 Schematic illustration of the regularization from α′-to α-form, the melting of the α-form, and recrystallization/epitaxial growth on the oriented stereocomplex crystallites (β_c) form in the heating of a PLLA/PDLA blend sample ($X_D = 0.5$) (Zhang et al., 2007).

induction period (t_i) for spherulite growth (Tsuji and Tezuka, 2004). These results indicate that the numbers of spherulites of stereocomplex crystallites per unit area are larger with higher G and lower t_i values than those of the spherulites of homocrystallites. This resulted in enhanced overall crystallization rate of stereocomplex crystallites compared with that of homocrystallites.

Zhang and co-workers investigated the crystalline phase change of PLLA/PDLA blends with high molecular weights using FT-IR spectroscopy by following three phase-transitions: the transition of α′-form to α-form at 120°C, melting of α-form, and recrystallization/epitaxial growth of stereocomplex crystallites above the melting temperature of homocrystallites (>170–180°C) (Fig. 7-10) (Zhang et al., 2007). Zhang and co-workers and Sarasua and co-workers revealed the hydrogen bonding between methyl hydrogen (or α-hydrogen) and carbonyl oxygen, which is expected to enhance rapid spherulite formation and growth of PLA stereocomplex crystallites (Zhang et al., 2005b; Sarasua et al., 2005).

7.3 METHODS FOR INDUCING STEREOCOMPLEXATION

Homocrystallization dominates stereocomplex crystallization, when the molecular weight of PLLA and PDLA is elevated. Figure 7-11 shows the melting enthalpies (ΔH_m) of stereocomplex crystallites and homocrystallites when a casting method was used for the specimen preparation. Clearly, ΔH_m of stereocomplex crystallites and homocrystallites decreased and increased, respectively, with increasing molecular weight, and ΔH_m of the stereocomplex became lower than that of homocrystallites when the weight-average molecular weight (M_w) increased above 3×10^5 g/mol (Tsuji et al., 1991a). The critical molecular weight, below which only stereocomplex crystallites are formed depends on the method and conditions of material preparation. Normally, the critical molecular weight is lower for melt processing than for solution processing (nonsolvent precipitation and solution casting), and higher for nonsolvent precipitation than for solution casting (Tsuji et al., 1991a; Tsuji and Ikada, 1993). Duan and co-workers reported the M_w dependence of stereocomplex formation for Langmuir monolayers on water (Duan et al., 2006). The result is similar to that for as-cast or melt-crystallized blends. PLLA and PDLA polymer pairs having high

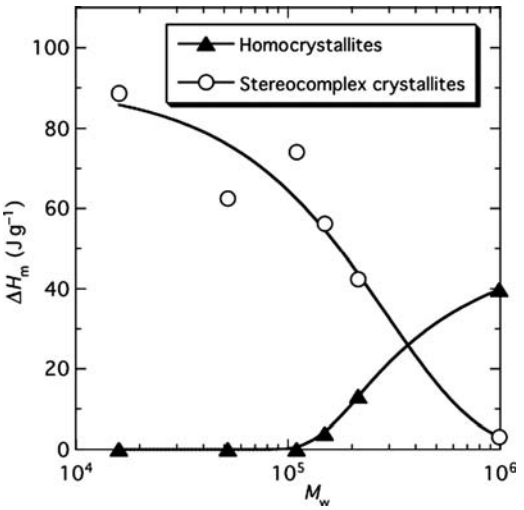

Fig. 7-11 Melting enthalpies (ΔH_m) of stereocomplex crystallites and homocrystallites for as-cast PLLA/PDLA blend films ($X_D = 0.5$) as a function of weight-average molecular weight (M_w) (Tsuji et al., 1991a).

molecular weights are required for high mechanical performance, whereas stereocomplex is readily formed when the molecular weight of either PLLA or PDLA is low. Therefore, the selection of processing method and conditions is crucial to resolve the conflict if high-molecular-weight PLLA/PDLA blend materials are required to contain only stereocomplex crystallites.

One method for enhancing stereocomplex formation is to increase the chain orientation of PLLA/PDLA (Tsuji et al., 1991a, 1994; Takasaki et al., 2003; Furuhashi et al., 2006, 2007; Sawai et al., 2006). This may be effected by the increased interaction between PLLA and PDLA chains due to shearing forces or thermal drawing. A novel method was developed to prepare well-stereocomplexed PLA materials by the use of electrospinning (i.e., by electrostatically induced high shearing force) of PLLA/PDLA concentrated solutions. The formation of homocrystallites was suppressed, while that of stereocomplex crystallites was enhanced (Tsuji et al., 2006a). This study further revealed that nano-order stereocomplex fibers could be formed by electrospinning, as shown in Fig. 7-12. On the other hand, stereocomplexation occurred upon compression of a monolayer of PLLA/PDLA blend films (Bourque et al., 2001; Pelletier and Pézolet, 2004). Study of the structural change of Langmuir films of PLLA/PDLA by the use of surface-pressure measurement and polarization modulation infrared reflecting-absorption spectroscopy (PM-IRRAS) indicated that a stereocomplex bilayer in equilibrium with the monolayer was formed at the air–water interface upon compression. Serizawa and co-workers reported that stepwise alternate immersion of a quartz crystal microbalance (QCM) substrate into respective acetonitrile solutions of PLLA and PDLA gave rise to stereocomplexation (Serizawa et al., 2003). They also indicated that the assembly of PLLA

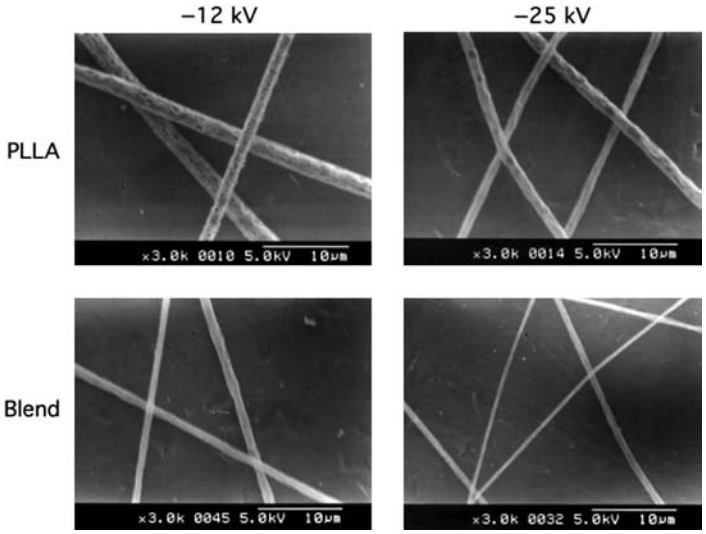

Fig. 7-12 SEM images of PLLA ($X_D = 0$) and PLLA/PDLA ($X_D = 0.5$) fibers electrospun at applied voltages of −12 and −25 kV (Tsuji et al., 2006a).

could grow epitaxially on the surface of stereocomplex crystallites, as shown also by Brochu et al. (1995).

A novel method was proposed by Spinu and co-workers for stereocomplexation between PLLA and PDLA. They conducted polymerization of LLA and DLA in the presence of PDLA and PLLA by mixing LLA and PDLA (or DLA and PLLA) (Spinu et al., 1996). This method successfully formed well-stereocomplexed PLA structures. In the strict sense, this method may not be identified as "template polymerization" (Challa and Tan, 1981), but it effectively utilizes the fact that polymerized chains have a strong interaction with the template chains.

Low-molecular-weight stereoblock PLA was incorporated in a 1 : 1 blend system of PLLA and PDLA having high molecular weights, acting as a compatibilizer to enhance stereocomplex formation (Fukushima et al., 2007).

7.4 PHYSICAL PROPERTIES

Physical properties of PLLA, PDLLA, and PLA stereocomplex are given in Table 7-2 (Tsuji, 2002a), together with those of poly((*R*)-3-hydroxybutyrate) (R-PHB), poly(ε-caprolactone) (PCL), and poly(glycolide) (PGA). The glass transition and melting of PLLA occur at 60°C and 180°C, respectively. As shown in Fig. 7-7, the T_m of the stereocomplex crystallites (220–230°C) was higher by about 50°C than that of homocrystallites of PLLA or PDLA (170–180°C). When stereocomplex formation takes place in concentrated PLA solutions, the stereocomplex microcrystallites formed serve as crosslinks accompanying a dramatic increase in solution viscosity and

finally a three-dimensional gel is formed (Tsuji et al., 1991b; Tsuji and Ikada, 1999). Such a viscosity increase or gelation was also reported for blends made from various block and graft copolymers containing LLA or DLA chains and hydrophilic chains in aqueous media (Lim et al., 2000; De Jong et al., 2000, 2001a, b, 2002; Fujiwara et al., 2001; Watanabe et al., 2002a, b; Watanabe and Ishihara, 2003; Li and Vert, 2003; Li, 2003; Mukose et al., 2004; Hennink et al., 2004; van Nostrum, 2004; Hiemstra et al., 2006).

The tensile properties of PLA were reported to be enhanced by stereocomplex formation. For M_w exceeding 1×10^5 g/mol, tensile strength, Young's modulus, and elongation-at-break of PLLA/PDLA films were much higher than those of pure PLLA and PDLA films (Fig. 7-13) (Tsuji and Ikada, 1999). As noted above, the stereocomplex crystallites can act as crosslinks and the well-stereocomplexed materials reveal higher mechanical performance than the nonstereocomplexed materials (Fig. 7-14) (Tsuji and Ikada, 1999). Even in the melt state, PLLA and PDLA chains have a strong interaction with each other, resulting in high thermal stability, as traced by thermogravimetric isothermal measurements in the temperature range 230–250°C (Tsuji and Fukui, 2003). It was also found that PLLA/PDLA films had a lower water vapor transmission rate than pure PLLA and PDLA films (Tsuruno and Tsuji, 2007). The differences in the rates between blend and nonblended films were higher for amorphous than for crystallized films. These results reflect that the interaction is stronger between different polymer chains than between the same polymer chains.

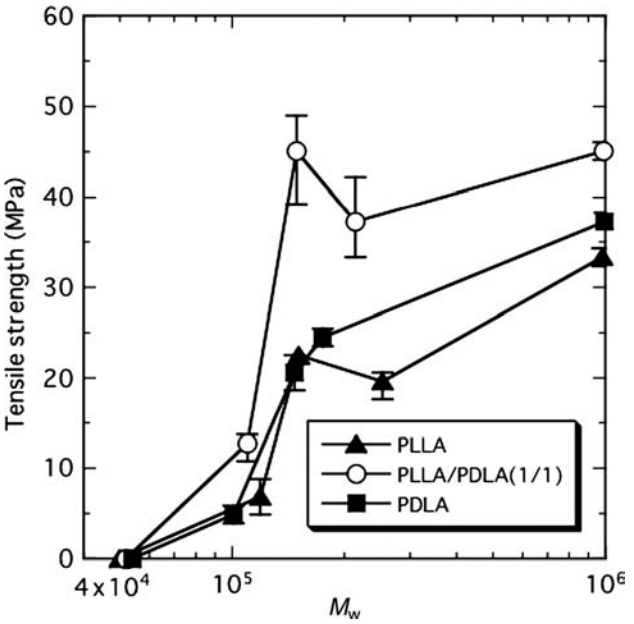

Fig. 7-13 Tensile strength of as-cast pure PLLA ($X_D = 0$), PDLA ($X_D = 1$), and PLLA/PDLA blend ($X_D = 0.5$) films as a function of M_w (Tsuji and Ikada, 1999).

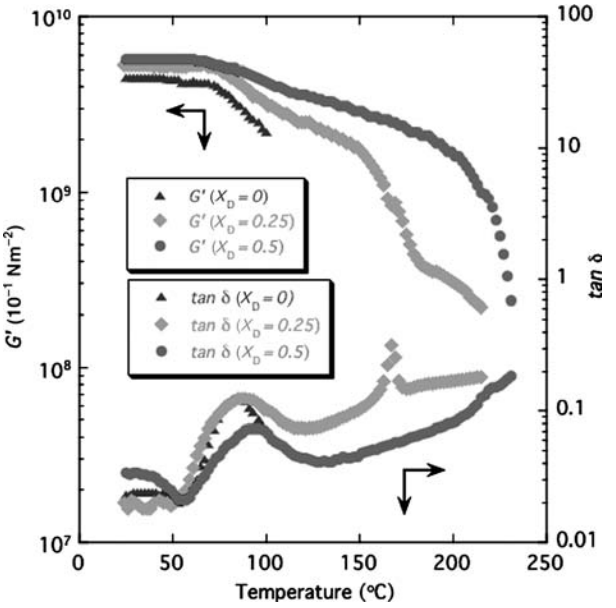

Fig. 7-14 Storage modulus (G') and loss tangent (*tan* δ) for PLLA ($X_D = 0$) and PLLA/PDLA blend ($X_D = 0.25$ and 0.5) films (Tsuji and Ikada, 1999).

7.5 BIODEGRADATION

Stereocomplexed PLA has a higher hydrolytic degradation resistance than nonblended PLLA or PDLA when they undergo hydrolytic degradation in phosphate-buffered solution at pH 7.4 and 37°C (Fig. 7-15) (Tsuji, 2000). It is surprising that although the decrease in tensile strength of nonblended specimens started at 4 months, stereocomplex specimens maintained their initial tensile strength for as long as 16 months. Similarly, De Jong and co-workers studied hydrolytic degradation of solution-cast LLA oligomers (degree of polymerization (DP) = 7 lactyl units) and the stereocomplex of LLA and DLA oligomers (DP = 7 lactyl units) at pH 7 and 37°C (De Jong et al., 2001a). They showed that the fraction of the LLA oligomer remaining approached zero within 4 h, whereas 50% of the stereocomplex remained even after 96 h of degradation. Although the LLA oligomer and stereocomplex are amorphous and crystalline, respectively, the observed results are in agreement with those for nonoligomeric PLA (Tsuji, 2000).

Stereocomplex crystallization must disturb the hydrolytic degradation of stereocomplexed specimens compared to that of nonblended PLA specimens, in spite of predominant hydrolytic degradation in the amorphous region between the stereocomplex crystalline regions. This means that PLLA and PDLA chains should have a strong interaction between them even when they are in the amorphous state, as suggested by the aforementioned thermal degradation results (Tsuji and Fukui, 2003). To confirm this assumption, various types of equimolarly blended specimens

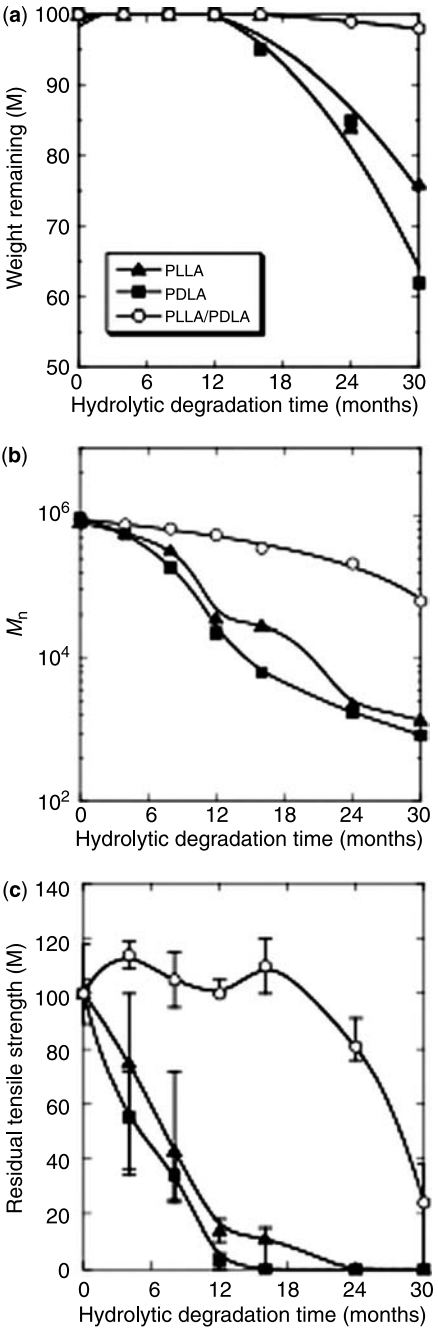

Fig. 7-15 Residual tensile strength (a), Young's modulus (b), and elongation-at-break (c) of PLLA ($X_D = 0$), PDLA ($X_D = 1$), and PLLA/PDLA blend ($X_D = 0.5$) films, as a function of hydrolytic degradation time (Tsuji, 2000).

were prepared from PLLA and PDLA—amorphous (Tsuji, 2002b) and homocrystallized (Tsuji, 2003)—and their hydrolytic degradation was carried out in phosphate-buffered solution at pH 7.4 and 37°C, together with nonblended PLLA and PDLA specimens. It was found that hydrolytic degradation of the blended specimens was retarded compared with that of the nonblended specimens, irrespective of their state (amorphous or homocrystallized), supporting the above hypothesis. Moreover, hydrolytic degradation of stereocomplexed fibers and films revealed that the morphology of the stereocomplexed materials had crucial effects on their hydrolytic degradation rate (Tsuji and Suzuki, 2001). Karst and Yang studied the molecular modeling of PLLA/PDLA blends, PLLA, and PDLA and found that hydrogen-bonding and dipole–dipole interactions were higher for PLLA/PDLA blends than for pure PLLA or PDLA, resulting in a higher hydrolytic degradation resistance of PLLA/PDLA blends (Karst and Yang, 2006). Possibly, hydrogen-bonding has a greater effect than the dipole–dipole interactions on the resistance to hydrolytic degradation.

Stereocomplexation between enantiomeric LLA and DLA unit sequences has been reported to retard hydrolytic degradation, for instance, of poly[2-hydroxyethyl methacrylate-*graft*-oligo(lactide)] (Lim et al., 2000) and A-B-A triblock copolymers of PLA (A) with poly(sebacic acid) (PSA) (B) (Slivniak and Domb, 2002). De Jong and co-workers indicated further that hydrolytic degradation of stereocomplex hydrogels from dextran (DS = 3–12)-*graft*-LLA and DLA oligomers (DP = 6–12 lactyl units) depended on the number of lactate grafts (DS), the length (DP) and polydispersity of the grafts, and the initial water content, with the hydrolytic degradation time varying from 1 to 7 days (De Jong et al., 2001b). van Nostrum and co-workers also showed that the hydrolytic degradation time of stereocomplex hydrogels from poly(2-hydroxypropyl methacrylamide) (pHPMAm)-*graft*-LLA and DLA oligomers could be readily tailored from 1 week to almost 3 weeks by changing the grafting density of the polymers and the structure of the terminal groups of side-chains (van Nostrum et al., 2004).

Another example was presented by proteinase K-catalyzed enzymatic degradation of PLLA/PDLA blends (Tsuji and Miyauchi, 2001a). Proteinase K is an endoprotease having broad specificity but with preference for the cleavage of the peptide bond C-terminal to aliphatic and aromatic amino acids, especially alanine (Sweeney and Walker, 1993). Similarity in chemical structures between lactic acid and alanine is expected to induce the proteinase K-catalyzed degradation of the C-terminal of PLLA or L-lactyl unit sequences. As is known, proteinase K can catalyze hydrolytic degradation of L-lactyl chains in the amorphous region (Tsuji and Miyauchi, 2001b, c). The proteinase K-catalyzed enzymatic degradation rate (R_{ED}) of PLLA/PDLA blends is plotted as a function of X_D in Fig. 7-16 (Tsuji and Miyauchi, 2001a). Proteinase K catalyzed the cleavage of L-lactyl unit sequences, when the average L-lactyl unit sequence length (l_L) was 4 units, and R_{ED} decreased with a decrease in l_L. Therefore, PLLA ($l_L = 57.1$) can be degraded in the presence of proteinase K, whereas degradation of PDLA ($l_L = 0$) is not catalyzed. In this study, the specimens were made amorphous to exclude the effects of highly ordered

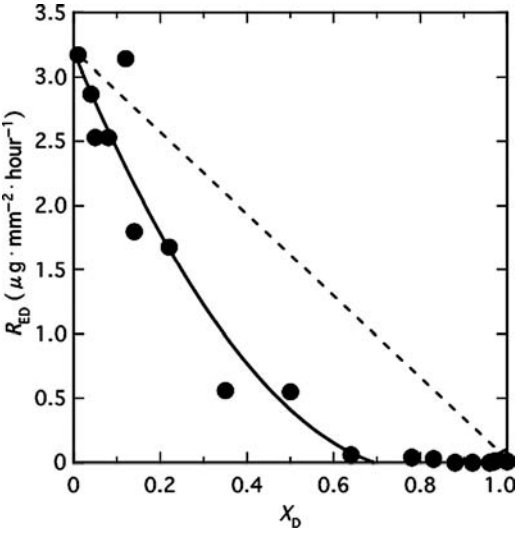

Fig. 7-16 Proteinase K-catalyzed enzymatic degradation rate (R_{ED}) of PLLA/PDLA blend films as a function of X_D (Tsuji and Miyauchi, 2001a).

structure such as crystallinity. As is seen in Fig. 7-16, R_{ED} of PLLA/PDLA blends is much lower than the expected, reflecting the mutual miscibility of PLLA and PDLA and the PDLA disturbance of enzymatic degradation of PLLA in the blends. If PDLA and PLLA were completely phase-separated, such disturbance would not be observed. Lee and co-workers also reported the disturbed proteinase K-catalyzed enzymatic degradation of PLLA/PDLA stereocomplex monolayer films compared with that of pure PLLA or PDLA monolayer film (Lee et al., 2005). However, in this case it seems difficult to define "stereocomplex" for the monolayer film.

7.6 APPLICATIONS

7.6.1 Biodegradable Films

Biodegradable PLA-based stereocomplex films can be prepared by a solution-casting method with organic solvents such as chloroform and methylene chloride (Murdoch and Loomis, 1988; Tsuji et al., 1991c; Tsuji and Ikada, 1999). In this method, the molecular weight of L-lactyl and D-lactyl unit sequences as well as the solvent evaporation rate are crucial. If the molecular weight and solvent evaporation rate are too high, stereocomplex formation is disturbed, resulting in formation of films containing a relatively large amount of homocrystallites or having low crystallinity (Tsuji et al., 1991c; Tsuji and Ikada, 1999). Although PLA stereocomplex films can also be prepared by a melt-molding method, it should be noted that the critical molecular weight of PLLA and PDLA, below which only stereocomplex crystallites

TABLE 7-2 Physical Properties of Some Biodegradable Aliphatic Polyesters (Tusji, 2002a)

Property	Polymer				
	PLLA	PLA Stereocomplex	PCL	R-PHB	PGA
T_m (°C)	170–190	220–230	60	180	225–230
T_m^0 (°C)	205–215	279	71, 79	188, 197	–
T_g (°C)	50–65	65–72	−60	5	40
ΔH_m^0 (J/g)	93, 135, 142, 203	142	142	146	180–207
Density (g/cm^3)	1.25–1.29	–	1.06–1.13	1.177–1.260	1.50–1.69
Solubility parameter (δ_p) (25°C) [(J/cm^3)$^{0.5}$]	19–20.5, 22.7	–	20.8	20.6	–
$[\alpha]_{589}^{25}$ in chloroform (25°C) (deg dm^{-1} g^{-1} cm^3)	-155 ± 1	–	0	+44[a]	–
WVTR[b] (g m^2 day^{-1})	82–172	–	177	13[c]	–
Tensile strength[d] (GPa)	0.12–2.3	0.92	0.1–0.8	0.18–0.20	0.08–1
Young's modulus[d] (GPa)	7–10	8.6	–	5–6	4–14
Elongation-at-break[d] (%)	12–26	30	20–120	50–70	30–40

[a] 300 nm, 23°C.
[b] Water vapor transmission rate at 25°C.
[c] P(HB-HV) (94/6).
[d] Oriented fiber.

are formed, decreases dramatically compared with that in the solution-casting method (Tsuji and Ikada, 1993). This indicates the difficulty of preparing well-stereocomplexed PLA with high molecular weights.

7.6.2 Biodegradable Fibers

Murdoch and Loomis 1988 prepared melt-spun PLA stereocomplex fibers from equimolar mixtures of PLLA and PDLA, while Tsuji and co-workers obtained wet- and dry-spun PLA stereocomplex fibers (Tsuji et al., 1994) from mixed chloroform solutions of equimolar PLLA and PDLA. The former study did not estimate the fraction of stereocomplex crystallites and homocrystallites (Murdoch and Loomis, 1988), whereas the latter estimated the fraction by DSC to reveal that hot-drawing of as-spun fibers increased the amount of stereocomplex crystallites but reduced that of homocrystallites, resulting in formation of fibers with stereocomplex as the main crystalline type (Tsuji et al., 1994). The PLA stereocomplex fibers used by Tsuji and Suzuki for hydrolytic degradation experiments were prepared by melt-spinning and subsequent two-stage hot-drawing, and contained only stereocomplex crystallites but no homocrystallites (Tsuji and Suzuki, 2001).

Takasaki and co-workers revealed that stereocomplexation was favored in melt-spinning from equimolar mixtures of PLLA and PDLA if the spinning was conducted under conditions of higher take-up velocity, lower throughput rate, and lower extrusion temperature (Takasaki et al., 2003). This finding suggests that these conditions can enhance the orientation-induced crystallization of the stereocomplex, as described above (Tsuji et al., 1994; Tsuji and Suzuki, 2001). They also confirmed that drawing at lower temperature and annealing between the T_m values of stereocomplex crystallites and homocrystallites enhanced stereocomplexation. This is in agreement with the above findings (Murdoch and Loomis, 1988; Tsuji and Ikada, 1993). The maximum tensile strength and Young's modulus were respectively 530 MPa and 7.4 GPa for melt-spun and drawn stereocomplex fibers (Murdoch and Loomis, 1988), 920 MPa and 8.6 GPa for solution-spun and drawn stereocomplex fibers (Tsuji et al., 1994), and 400 MPa and 4.7 GPa for as-spun stereocomplex fibers (Takasaki et al., 2003). These values are much lower than the maximum tensile strength and Young's modulus (2.1 GPa and 16 GPa) of melt-spun and drawn PLLA fibers (Leenslag and Pennings, 1987).

7.6.3 Biodegradable Microspheres for Drug Delivery Systems

Loomis and Murdoch (1990) prepared injectable stereocomplex microspheres containing a naltrexone base using an oil-in-water (O/W) solvent-evaporation method (O: methylene chloride; W: water with a surfactant). The release of naltrexone was delayed by a lag time of 200, 230, and 240 h in water, acid, and buffer solutions, respectively. After the lag, drug release occurred with zero-order kinetics up to 450 h with 46%, 48%, and 35% of the drug released in water, acid, and buffer solutions, respectively. In contrast, de Jong et al. (2001b) showed that stereocomplex hydrogels prepared from dextran (DS = 3–12)-*graft*-LLA and DLA oligomers

(DP = 6–12 lactyl units) released entrapped model proteins (IgG and lysozyme) during a period of 6 days.

Slager and Domb formulated "heterostereocomplex" drug delivery system (DDS) particles from L-configured peptides such as insulin with PDLA, PDLA-*b*-PEG, PDLA-*b*-PEG/PDLA, PLLA/PDLA, or PLLA-*b*-PEG/PDLA-*b*-PEG (Slager and Domb, 2002). Strong physical entrapment of peptides by the DLA unit sequence resulted in retarded release of the peptides. They also prepared heterostereocomplex DDS particles from an L-configured leuprolide and PDLA (Slager and Domb, 2003b, c; 2004). Various factors affected the release of leuprolide from the hetero-stereocomplex particles. The release rate of leuprolide from the particles increased with the decreasing molecular weight of PDLA and the increasing weight fraction of leuprolide. Continuous release of leuprolide over 100 days was observed at certain stereocomplex compositions (Slager and Domb, 2003b).

7.6.4 Biodegradable Hydrogels

Stereocomplexed PLA hydrogels can be prepared in aqueous media by blending block or graft copolymers possessing hydrophilic segments and L-lactyl or D-lactyl unit sequences. Such stereocomplex hydrogels were reported for enantiomeric A-B diblock and A-B-A triblock copolymers (Fujiwara et al., 2001; De Jong et al., 2002; Li and Vert, 2003; Li, 2003) and B-A-B triblock copolymers (Mukose et al., 2004) of PLA (A) with PEG (B); for enantiomeric graft copolymers of poly[2-hydroxyethyl methacrylate-*graft*-oligo(lactide)] (Lim et al., 2000); poly(2-hydroxy-propyl methacrylamide) (pHPMAm)-*graft*-LA oligomers (van Nostrum et al., 2004) and dextran-*graft*-LA oligomers (De Jong et al., 2000, 2001a,b, 2002; Hennink et al., 2004). Hiemstra and co-workers synthesized PEG-$(PLLA)_8$ and PEG-$(PDLA)_8$ star block copolymers with high storage moduli up to 14 kPa by mixing aqueous solutions with equimolar amounts of PEG-$(PLLA)_8$ and PEG-$(PDLA)_8$ (Hiemstra et al., 2006).

Watanabe, Ishihara and co-workers prepared porous stereocomplexed PLA films from graft-type copolymers containing LLA unit sequences or DLA sequences as side-chains (PMBLLA and PMBDLA, respectively), using an extraction method with water-soluble particles of NaCl (Watanabe et al., 2002a,b; Watanabe and Ishihara 2003). They showed that the cell adhesion and morphology of the porous scaffolds were correlated with the PLLA or PDLA content and the 2-methacryloyloxy-ethylphosphorylcholine (MPC) unit content, respectively (Watanabe et al., 2002b). Fibroblast cells adhered on the surface and intruded into the scaffolds through the connected pores after 24 h. The cell morphology became round from spreading when the PLLA or PDLA content in the scaffolds decreased.

7.6.5 Nucleation Agents

As reported in many articles (Brochu et al., 1995; Schmidt and Hillmyer, 2001; Yamane and Sasai, 2003; Anderson and Hillmyer 2006; and Tsuji et al. 2006b,c), stereocomplex crystallites formed by addition of small amounts of PDLA to

PLLA act as heterogeneous nucleation sites for PLLA crystallization, and PLLA homocrystallites are formed epitaxially on the stereocomplex crystallites. Such nucleation agents increase the number of PLLA spherulites per unit volume and the total crystallization rate, but do not alter the spherulite growth rate (Tsuji et al., 2006b, c).

REFERENCES

Abe H, Kikkawa Y, Inoue Y, Doi Y. 2001. Morphological and kinetic analyses of regime transition for poly((*S*)-lactide) crystal growth. *Biomacromolecules* 2:1007–1014.

Albertsson A-C, editor. 2002. *Degradable Aliphatic Polyesters* (Advances in Polymer Science, vol. 157). Berlin: Springer.

Anderson KS, Hillmyer MA. 2006. Melt preparation and nucleation efficiency of polylactide stereocomplex crystallites. *Polymer* 47:2030–2035.

Auras R, Harte B, Selke S. 2004. An overview of polylactides as packaging materials. *Macromol Biosci* 4:835–864.

Bourque H, Laurin I, Pézolet M. 2001. Investigation of the poly(L-lactide)/poly(D-lactide) stereocomplex at the air–water interface by polarization modulation infrared reflection absorption spectroscopy. *Langmuir* 17:5842–5849.

Brizzolara D, Cantow H-J, Diederichs K, Keller E, Domb AJ. 1996. Mechanism of stereocomplex formation between enantiomeric poly(lactide)s. *Macromolecules* 29:191–197.

Brochu S, Prud'homme RE, Barakat I, Jérôme R. 1995. Stereocomplexation and morphology of polylactides. *Macromolecules* 28:5230–5239.

Cartier L, Okihara T, Ikada Y, Tsuji H, Puiggali J, Lotz B. 2000. Epitaxial crystallization and crystalline polymorphism of polylactides. *Polymer* 41:8909–8919.

Challa G, Tan YY. 1981. Template polymerization. *Pure Appl Chem* 53:627–641.

Coombes AGA, Meikle MC. 1994. Resorbable synthetic polymers as replacements for bone graft. *Clin Mater* 17:35–67.

De Jong SJ, DeSmedt SC, Wahls MWC, Demeester J, Kettenes-van den Bosch JJ, Hennink WE. 2000. Novel self-assembled hydrogels by stereocomplex formation in aqueous solution of enantiomeric lactic acid oligomers grafted to dextran. *Macromolecules* 33:3680–3686.

De Jong SJ, van Eerdenbrugh B, van Nostrum CF, Kettenes-van den Bosch JJ, Hennink WE. 2001a. Biodegradable hydrogels based on stereocomplex formation between lactic acid oligomers grafted to dextran. *J Control Release* 72:47–56.

De Jong SJ, DeSmedt SC, Demeester J, van Nostrum CF, Kettenes-van den Bosch JJ, Hennink WE. 2001b. Physically crosslinked dextran hydrogels by stereocomplex formation of lactic acid oligomers: degradation and protein release behavior. *J Control Release* 71:261–275.

De Jong SJ, van Nostrum CF, Kroon-Batenburg LMJ, Kettenes-van den Bosch JJ, Hennink WE. 2002. Oligolactate-grafted dextran hydrogels: Detection of stereocomplex crosslinks by X-ray diffraction. *J Appl Polym Sci* 86:289–293.

De Santis P, Kovacs AJ. 1968. Molecular conformation of poly(*S*-lactic acid). *Biopolymer* 6:299–306.

Di Lorenzo ML. 2005. Crystallization behavior of poly(L-lactic acid). *Eur Polym J* 41:569–575.

Doi Y, Fukuda K, editors. 1994. *Biodegradable Plastics and Polymers*. Amsterdam: Elsevier.

Duan Y, Liu J, Sato H, Zhang J, Tsuji H, Ozaki Y, Yan S. 2006. Molecular weight dependence of the poly(L-lactide)/poly(D-lactide) stereocomplex at the air–water interface. *Biomacromolecules* 7:2728–2735.

Fujiwara T, Mukose T, Yamaoka T, Yamane H, Sakurai S, Kimura Y. 2001. Novel thermoresponsive formation of a hydrogel by stereo-complexation between PLLA-PEG-PLLA and PDLA-PEG-PDLA block copolymers. *Macromol Biosci* 1:204–208.

Fukushima K, Chang Y-H, Kimura Y. 2007. Enhanced stereocomplex formation of poly(L-lactic acid) and poly(D-lactic acid) in the presence of stereoblock poly(lactic acid). *Macromol Biosci* 7:829–835.

Furuhashi Y, Kimura Y, Yoshie N, Yamane H. 2006. Higher-order structures and mechanical properties of stereocomplex-type poly(lactic acid) melt spun fibers *Polymer* 47:5965–5972.

Furuhashi Y, Kimura Y, Yamane H. 2007. Higher order structural analysis of stereocomplex-type poly(lactic acid) melt-spun fibers. *J Polym Sci Part B: Polym Phys* 45:218–228.

Garlotta D. 2001. A literature review of poly(lactic acid). *J Polym Environ* 9:63–84.

Gupta B, Revagade N, Hilborn J. 2007. Poly(lactic acid) fiber: An overview. *Prog Polym Sci* 32:455–482.

Hartmann MH. 1998. In: Kaplan DL, editor. *Biopolymers from Renewable Resources*. Berlin: Springer; 1998. p. 367–411.

Hennink WE, De Jong SJ, Bos GW, Veldhuis TFJ, van Nostrum CF. 2004. Biodegradable dextran hydrogels crosslinked by stereocomplex formation for the controlled release of pharmaceutical proteins. *Int J Pharm* 277:99–104.

Hiemstra C, Zhong Z, Li L, Dijkstra PJ, Feijen J. 2006. In-situ formation of biodegradable hydrogels by stereocomplexation of PEG-$(PLLA)_8$ and PEG-$(PDLA)_8$ star block copolymers. *Biomacromolecules* 7:2790–2795.

Hoogsteen W, Postema AR, Pennings AJ, ten Brinke G, Zugenmaier P. 1990. Crystal structure, conformation, and morphology of solution-spun poly(L-lactide) fibers. *Macromolecules* 23:634–642.

Ikada Y, Tsuji H. 2000. Biodegradable polyesters for medical and ecological applications. *Macromol Rapid Commun* 21:117–132.

Ikada Y, Jamshidi K, Tsuji H, Hyon S-H. 1987. Stereocomplex formation between enantiomeric poly(lactides). *Macromolecules* 20:904–906.

Kalb B, Pennings AJ. 1980. General crystallization behaviour of poly(L-lactic acid). *Polymer* 21:607–612.

Kawai T, Rahman N, Matsuba G, Nishida K, Kanaya T, Nakano M, Okamoto H, Kawada J, Usuki A, Honma N, Nakajima K, Matsuda M. 2007. Crystallization and melting behavior of poly(L-lactic acid). *Macromolecules* 40:9463–9469.

Karst D, Yang Y. 2006. Molecular modeling study of the resistance of PLA to hydrolysis based on the blending of PLLA and PDLA. *Polymer* 47:4845–4850.

Kharas GB, Sanchez-Riera F, Severson DK. 1994. In Mobley DP, editors. Plastics from Microbes. New York: Hanser Publishers. p. 93–137.

Kobayashi J. Asahi T, Ichiki M, et al. 1995. Structural and optical properties of poly lactic acids. *J Appl Phys* 77:2957–2973.

Lee W-K, Iwata T, Gardella JA, Jr. 2005. Hydrolytic behavior of enantiomeric poly(lactide) mixed monolayer films at the air/water interface: stereocomplexation effects. *Langmuir* 21:11180–11184.

Leenslag JW, Pennings AJ. 1987. High-strength poly(L-lactide) fibres by a dry-spinning/hot-drawing process. *Polymer* 28:1695–1702.

Li S. 2003. Bioresorbable hydrogels prepared through stereocomplexation between poly(L-lactide) and poly(D-lactide) blocks attached to poly(ethylene glycol). *Macromol Biosci* 3:657–661.

Li S, Vert M. 2003. Synthesis, characterization, and stereocomplex-induced gelation of block copolymers prepared by ring-opening polymerization of L(D)-lactide in the presence of poly(ethylene glycol). *Macromolecules* 36:8008–8014.

Lim DW, Choi SH, Park TG. 2000. A new class of biodegradable hydrogels stereocomplexed by enantiomeric oligo(lactide) side chains of poly(HEMA-γ-OLA)s. *Macromol Rapid Commun* 21:464–471.

Loomis GL, Murdoch JR. 1990. Polylactide compositions. U.S. Patent, 4,902,515.

Mukose T, Fujiwara T, Nakano J, et al. 2004. Hydrogel formation between enantiomeric B-A-B-type block copolymers of polylactides (PLLA or PDLA: A) and Polyoxyethylene (PEG: B); PEG-PLLA-PEG and PEG-PDLA-PEG4. *Macromol Biosci* 361–367.

Murdoch JR, Loomis GL. 1988. Polylactide compositions. U.S. Patent, 4,719,246.

Okihara T. Tsuji M, Kawaguchi A, et al. 1991. Crystal structure of stereocomplex of poly(L-lactide) and poly(D-lactide). *Macomol Sci-Phys B* 30:119–140.

Pan P, Zhu B, Kai W, Dong T, Inoue T. 2008. Effect of crystallization temperature on crystal modifications and crystallization kinetics of poly(L-lactide). *J Appl Polym Sci* 107:54–62.

Pelletier I, Pézolet M. 2004. Compression-induced stereocomplexation of polylactides at the air/water interface. *Macromolecules* 37:4967–4973.

Puiggali J, Ikada Y, Tsuji H, Cartier L, Okihara T, Lotz B. 2000. The frustrated structure of poly(L-lactide). *Polymer* 41:8921–8930.

Sarasua J-R, López Rodrígues N, López Arraiza A, Meaurio E. 2005. Stereoselective crystallization and specific interactions in polylactides. *Macromolecules* 38:8362–8371.

Sawai D, Tamada M, Yokoyama T, Kanamoto T, Hyon S-H, Moon S. 2007. Stereocomplex crystal formation and development of morphology and mechanical property upon drawing of a blend of high molecular weight poly(L-lactic acid)/poly(D-lactic acid). *Sen'I Gakkaishi* 63:1–7.

Schmidt SC, Hillmyer MA. 2001. Polylactide stereocomplex crystallites as nucleating agents for isotactic polylactide. *J Polym Sci Part B: Polym Phys* 39:300–313.

Scott G, editor. 2002. *Biodegradable Polymers: Principles and Applications*, 2nd ed. Dordrecht: Kluwer Academic Publishers.

Serizawa T, Arikawa Y, Hamada K, et al. 2003. Alkaline hydrolysis of enantiomeric poly(lactide)s stereocomplex deposited on solid substrates, *Macromolecules* 36:1762–1765.

Slager J, Domb AJ. 2002. Stereocomplexes based on poly(lactic acid) and insulin: Formulation and release studies. *Biomaterials* 23:4389–4396.

Slager J, Domb AJ. 2003a. Biopolymer stereocomplexes. *Adv Drug Delivery Rev* 55:549–583.

Slager J, Domb AJ. 2003b. Heterostereocomplexes prepared from D-poly(lactide) and leuprolide. I. Characterization. *Biomacromolecules* 4:1308–1315.

Slager J, Domb AJ. 2003c. Heterostereocomplexes prepared from D-PLA and L-PLA and leuprolide. II. Release of leuprolide. *Biomacromolecules* 4:1316–1320.

Slager J, Domb AJ. 2004. Hetero-stereocomplexes of D-poly(lactic acid) and the LHRH analogue leuprolide. Application in controlled release. *Eur J Pharm Biopharm* 58:461–469.

Slivniak R, Domb AJ. 2002. Stereocomplexes of enantiomeric lactic acid and sebacic acid ester-anhydride triblock copolymers. *Biomacromolecules* 3:754–760.

Södergård A, Stolt M. 2002. Properties of lactic acid based polymers and their correlation with composition. *Prog Polym Sci* 27:1123–1163.

Spinu M, Jackson C, Keating MY, Gardner KH. 1996. Material design in poly(lactic acid) system: Block copolymers, star homo- and copolymers, and sereocomplexes. *J Macromol Sci-Pure Appl Chem* A33:1497–1530.

Sweeney PJ, Walker JM. 1993. Proteinase K. In: Burrell MM, editor. *Enzymes of Molecular Biology* (Methods in Molecular Biology, vol. 16). Totowa, NJ: Humana Press. p. 305–311.

Takasaki M, Ito H, Kikutani T. 2003. Development of stereocomplex crystal of polylactide in high-speed melt spinning and subsequent drawing and annealing processes. *J Macromol Sci Part B: Phys* B42:403–420.

Tsuji H. 2000. In vitro hydrolysis of blends from enantiomeric poly(lactide)s. Part 1. Well-stereocomplexed blend and non-blended films. *Polymer* 41:3621–3630.

Tsuji H. 2002a. Poly(lactide). In: Doi Y, Steinbüchel A. editors. *Polyesters III* (Biopolymers, vol. 4) Weinheim: Wiley-VCH. p. 129–177.

Tsuji H. 2002b. Autocatalytic hydrolysis of amorphous-made polylactides: effects of L-lactide content, tacticity, and enantiomeric polymer blending. *Polymer* 43:1789–1796.

Tsuji H. 2003. In vitro hydrolysis of blends from enantiomeric poly(lactide)s. Part 4: well-homo-crystallized blend and nonblended films. *Biomaterials* 24:537–547.

Tsuji H. 2005. Poly(lactide) stereocomplexes: formation, structure, properties, degradation, and applications. *Macromol Biosci* 5:569–597.

Tsuji H. 2007. Degradation of poly(lactide)-based biodegradable materials. In: Albertov LB editor. *Polymer Degradation and Stability Research Developments*. New York: Nova Science Book Publishers, p. 11–59.

Tsuji H, Fukui I. 2003. Enhanced thermal stability of poly(lactide)s in the melt by enantiomeric polymer blending. *Polymer* 44:2891–2896.

Tsuji H, Ikada Y. 1993. Stereocomplex formation between enantiomeric poly(lactic acid)s. 9. Stereocomplexation from the melt. *Macromolecules* 26:6918–6926.

Tsuji H, Ikada Y. 1995. Properties and morphologies of poly(L-lactide): 1. Annealing condition effects on properties and morphologies of poly(L-lactide). *Polymer* 36:2709–2716.

Tsuji H, Ikada Y. 1999. Stereocomplex formation between enantiomeric poly(lactic acid)s. XI. Mechanical properties and morphology. *Polymer* 40:6699–6708.

Tsuji H, Miyauchi S. 2001a. Enzymatic hydrolysis of poly(lactide)s: Effects of molecular weight, L-lactide content, and enantiomeric and diastereoisomeric polymer blending. *Biomacromolecules* 2:597–604.

Tsuji H, Miyauchi S. 2001b. Poly(L-lactide): VI. Effects of crystallinity on enzymatic hydrolysis of poly(L-lactide) without free amorphous region. *Polym Degrad Stab* 71:415–421.

Tsuji H, Miyauchi S. 2001c. Poly(L-lactide): 7. Enzymatic hydrolysis of free and restricted amorphous regions in poly(L-lactide) films with different crystallinities and a fixed crystalline thickness. *Polymer* 42:4463–4467.

Tsuji H, Suzuki M. 2001. In vitro hydrolysis of blends from enantiomeric poly(lactide)s. 2. Well-stereocomplexed fiber and film. *Sen'i Gakkishi* 57:198–202.

Tsuji H, Tezuka Y. 2004. Stereocomplex formation between enantiomeric poly(lactic acid)s. XII. Spherulite growth of low-molecular-weight poly(lactic acid)s. *Biomacromolecules* 5:1181–1186.

Tsuji H, Hyon S-H, Ikada Y. 1991a. Stereocomplex formation between enantiomeric poly(lactic acid)s. 4. Differential scanning calorimetric studies on precipitates from mixed solutions of poly(D-lactic acid) and poly(L-lactic acid). *Macromolecules* 24:5657–5662.

Tsuji H, Horii F, Hyon S-H, Ikada Y. 1991b. Stereocomplex formation between enantiomeric poly(lactic acid)s. 2. Stereocomplex formation in concentrated solutions. *Macromolecules* 24:2719–2724.

Tsuji H, Hyon S-H, Ikada Y. 1991c. Stereocomplex formation between enantiomeric poly(lactic acid)s. 3. Calorimetric studies on blend films cast from dilute solution. *Macromolecules* 24:5651–5656.

Tsuji H, Hyon S-H, Ikada Y. 1992. Stereocomplex formation between enantiomeric poly(lactic acid)s. 5. Calorimetric and morphological studies in the stereocomplex formed in acetonitrile solution. *Macromolecules* 25:2940–2946.

Tsuji H, Ikada Y, Hyon S-H, Kimura Y, Kitao T. 1994. Stereocomplex formation between enantiomeric poly(lactic acid)s. VIII. Complex fibers spun from mixed solution of poly(D-lactic acid) and poly(L-lactic acid); *J Appl Polym Sci* 51:337–344.

Tsuji H, Miyase T, Tezuka Y, Saha SK. 2005a. Physical properties and crystallization, and spherulite growth of linear and 3-arm poly(L-lactide)s. *Biomacromolecules* 6:244–254.

Tsuji H, Tezuka Y, Saha SK, Suzuki M, Itsuno S. 2005b. Spherulite growth of L-lactide copolymers: Effects of tacticity and comonomers. *Polymer* 46:4917–4927.

Tsuji H, Nakano M, Hashimoto M, Takashima Katsura K, Mizuno A. 2006a. Electrospinning of poly(lactic acid) stereocomplex nanofibers. *Biomacromolecules* 7:3316–3320.

Tsuji H, Takai H, Saha SK. 2006b. Isothermal and non-isothermal crystallization behavior of poly(L-lactic acid): Effects of stereocomplex as nucleating agent. *Polymer* 47:3826–3837.

Tsuji H, Takai H, Fukuda N, Takikawa H. 2006c. Non-isothermal crystallization behavior of poly(L-lactic acid) in the presence of various additives. *Macromol Mater Eng* 291:325–335.

Tsuruno T, Tsuji H. 2007. Water vapor permeability of poly(lactic acid) stereocomplex films. *Polym Prepr Japan* 56:2273.

van Nostrum CF, Veldhuis TFJ, Bos GW, Hennink WE. 2004. Tuning the degradation rate of poly(2-hydroxypropyl methacrylamide)-graft-oligo(lactic acid) stereocomplex hydrogels. *Macromolecules* 37:2113–2118.

Vert M, Schwarch G, Coudane JJ. 1995. Present and future of PLA polymers. *J Macromol Sci Pure Appl Chem* A32:787–796.

Watanabe J, Ishihara K. 2003. Higher water intrusion property on novel porous matrix composed of bioinspired polymer stereocomplex for tissue engineering. *Chem Lett* 32:192–193.

Watanabe J, Eriguchi T, Ishihara K. 2002a. Stereocomplex formation by enantiomeric poly(lactic acid) graft-type phospholipid polymers for tissue engineering. *Biomacromoleucles* 3:1109–1114.

Watanabe J, Eriguchi T, Ishihara K. 2002b. Cell adhesion and morphology in porous scaffold based on enantiomeric poly(lactic acid) graft-type phospholipid polymers. *Biomacromoleucles* 3:1375–1383.

Yamane H, Sasai K. 2003. Effect of the addition of poly(D-lactic acid) on the thermal property of poly(L-lactic acid). *Polymer* 44:2569–2575.

Yu L, Dean K, Li L. 2006. Polymer blends and composites from renewable resources. *Prog Polym Sci* 31:576–602.

Zhang J, Duan Y, Sato H, et al. 2005a. Crystal modifications and thermal behavior of poly(L-lactic acid) revealed by infrared spectroscopy. *Macromolecules* 38:8012–8021.

Zhang J, Sato H, Tsuji H, Noda I, Ozaki Y. 2005b. Infrared spectroscopic study of $CH_3 \cdots O=C$ interaction during the poly(L-lactide)/poly(D-lactide) stereocomplex formation. *Macromolecules* 38:1822–1828.

Zhang J, Tashiro K, Tsuji H, Domb AJ. 2007. Investigation of phase transitional behavior of poly(L-lactide)/poly(D-lactide) blend used to prepare the highly-oriented stereocomplex. *Macromolecules* 40:1049–1054.

CHAPTER 8

Polyhydroxyalkanoate Blends and Composites

GUO-QIANG CHEN

Multidisciplinary Research Center (MRC), Shantou University, Shantou, Guangdong, China; Department of Biological Sciences and Biotechnology, Tsinghua University, Beijing, China

RONG-CONG LUO

Multidisciplinary Research Center (MRC), Shantou University, Shantou, Guangdong, China

8.1 INTRODUCTION

Polyhydroxyalkanoates (PHAs) are a family of intracellular biopolymers synthesized by many bacteria as intracellular carbon and energy storage granules (Fig. 8-1). It is generally believed that PHA synthesis is promoted by unbalanced growth (Anderson and Dawes, 1990). The plastic-like properties and biodegradability of PHAs make them attractive as potential replacements for nondegradable polyethylene and polypropylene, as well as biodegradable and biocompatible biomaterials for implant purposes (Chen and Wu, 2005). Many efforts have been made to produce PHAs as environmentally degradable thermoplastics (Chen, 2003), including the large-scale production of poly-3-hydroxybutyrate (PHB) (Hrabak, 1992), copolyesters of 3-hydroxybutyrate and 3-hydroxyvalerate (PHBV) (Chen et al., 1991;

Biodegradable Polymer Blends and Composites from Renewable Resources. Edited by Long Yu

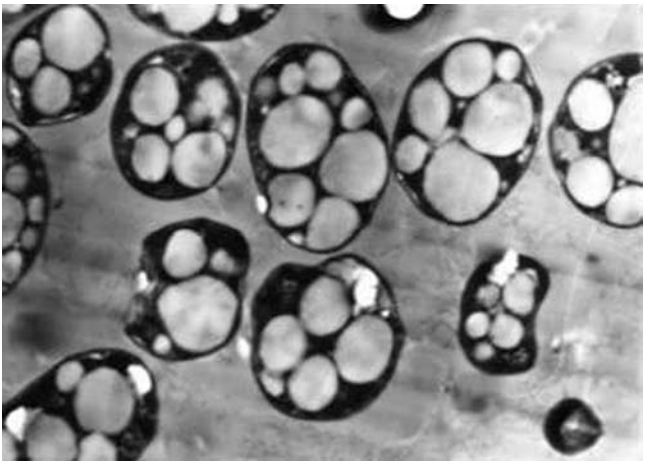

Fig. 8-1 Bacterial cells containing PHA granules imaged by scanning electron microscopy (Chen et al., 2000).

Byrom, 1992), copolyesters of 3-hydroxybutyrate and 3-hydroxyhexanoate (PHBHHx) (Chen et al., 2001), as well as medium-chain-length (mcl) PHA (Weusthuis et al., 2002) (Figs. 8-2 and 8-3).

PHB is the most common and lowest-cost PHA available but has the poorest properties for applications (Table 8-1) (Doi et al., 1995). Recently, a copolyester of 3-hydroxybutyrate and 4-hydroxybutyrate (P3HB4HB) was also produced by Tianjin Green Bioscience Co. Ltd in Tianjin (China) at one-tonne scale, allowing more investigation into this unique material.

As PHB is very brittle and prone to thermal degradation, it is necessary to improve its mechanical properties and processability through copolymerization or blending. In fact, since it is very difficult to develop new copolymers, blending with a second, already available, cheaper polymer has been attempted by many in the polymer research community.

There have been many reports on the blending of PHB with other biodegradable or nonbiodegradable polymers; these include poly(vinyl acetate) (PVAc) (Greco and Martuscelli, 1989; Kumagai and Doi, 1992a,b), poly(epichlorohydrin) (PECH) (Dubini et al., 1993; Sadocco et al., 1993), poly(vinyl alcohol) (PVA) (Azuma et al., 1992), atactic poly-[(*R*,*S*)-3-hydroxybutyrate] (Abe et al., 1995) and its block copolymer with poly(ethylene glycol) (P(*R*,*S*-HB-*b*-EG) (Kumagai and Doi,

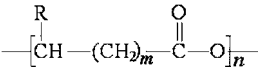

Fig. 8-2 General molecular structure of polyhydroxyalkanoates (PHAs). $m = 1$, 2, 3, with $m = 1$ the most common; n can range from 100 to several thousands. R is variable. When $m = 1$, $R = CH_3$, the monomer structure is 3-hydroxybutyrate; with $m = 1$ and $R = C_3H_7$, the monomer is a 3-hydroxyhexanoate monomer.

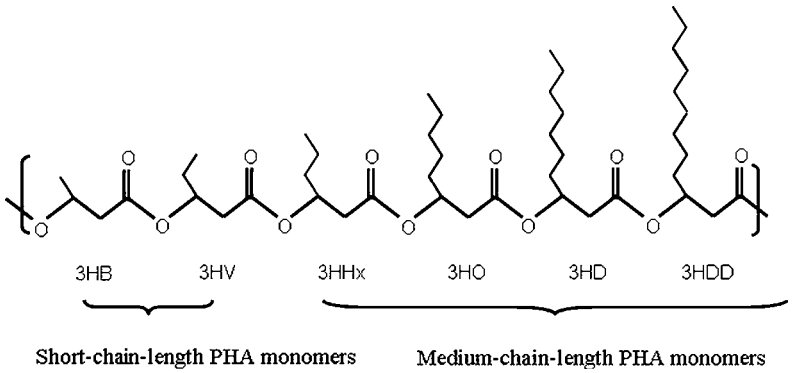

Fig. 8-3 Some commonly synthesized PHA monomers. Short-chain-length (scl) PHA monomers: 3HB, 3-hydroxybutyrate; 3HV, 3-hydroxyvalerate. Medium-chain-length PHA monomers: 3HHx, 3-hydroxyhexanoate; 3HO, 3-hydroxyoctanoate; 3HD, 3-hydroxydecanoate; 3HDD, 3-hydroxydodecanoate.

1993), poly(L-lactic acid-co-ethylene glycol-co-adipic acid) (Yoon et al., 1996), cellulose acetate butyrate (CAB) or cellulose acetate propionate (CAP) (Scandola et al., 1992), and poly(ethylene oxide) (PEO) (Avella and Martuscelli 1988; Kim et al., 1999). Poly(methyl methacrylate) (PMMA) is known to be immiscible with PHB at room temperature (Yoon et al., 1993); however, it is partially miscible in its molten state (Lotti et al., 1993). Immiscible blends have been prepared by mixing PHB with poly(1,4-butylene adipate) (PBA) (Kumagai and Doi, 1992a), PCL (Kumagai and Doi, 1992), poly(cyclohexyl methacrylate) (PCHMA) (Lotti et al., 1993), PHBV (Kumagai and Doi, 1992; Organ and Barham, 1993; Pearce and Marchessault, 1994; Gassner and Owen, 1996), and rubbers, such as

TABLE 8-1 Physical Properties of Various PHAs in Comparison with Conventional Plastics

Sample[a]	T_m (°C)	T_g (°C)	Tensile Strength (Mpa)	Elongation at Break (%)
PHB	177	4	43	5
P(HB-*co*-10% HV)	150	2	25	20
P(HB-*co*-20% HV)	135	−5	20	100
P(HB-*co*-10% HHx)	127	−1	21	400
P(HB-*co*-17% HHx)	120	−2	20	850
Polypropylene	170	–	34	400
Polystyrene	110	–	50	–
PET	262	69	56	7300
HDPE	135	–	29	–

[a]HV, 3-hydroxyvalerate; HHx, 3-hydroxyhexanoate; PET, poly(ethylene teraphthalate); HDPE, high-density polyethylene.

ethylene-propylene rubber (EPR) (Greco and Martuscelli, 1989; Abbate et al., 1991), ethylene-vinyl acetate (EVA) (Avella and Martuscelli, 1988; Abbate et al., 1991), modified EPR rubbers grafted with succinic anhydride (EPR-*g*-SA) or dibutyl maleate (EPR-*g*-DBM), or a modified EVA polymer containing OH groups (EVAL). Verhoogt and co-workers reviewed the properties and biodegradability of blends containing either PHB or PHBV (Verhoogt et al., 1994).

In this chapter, the blending of PHA with various polymers or additives is discussed.

8.2 PHA BLENDED WITH STARCH OR CELLULOSE

Starch is one of the cheapest biomaterials. If starch is mixable with PHB, it will help both reduction of the cost of PHB and improved PHB biodegradability. Godbole and co-workers (Godbole et al., 2003) studied the compatibility of PHB with starch. They indicated that blend films had a single glass transition temperature for all the proportions of PHB : starch tested; all combinations were found to be crystalline. The tensile strength was optimum for the PHB : starch ratio of 0.7 : 0.3 (wt/wt) (Table 8-2).

The results indicate that blending of starch with PHB in a ratio of 30 : 70 could be beneficial for cost reduction with improved properties over the virgin PHB. This blend material might also be used as a coating material on paper or cardboard used for food packaging etc. (Godbole et al., 2003) (Table 8-2).

The thermal behavior and phase morphology of PHB and starch acetate (SA) blends have been studied and they were found to be immiscible. The melting temperatures of PHB in the blends showed some shift with increase of SA content. The melting enthalpy of the PHB phase in the blend was close to the value for pure PHB. The glass transition temperatures of PHB in the blends remained constant at 9°C. The FTIR absorptions of hydroxyl groups of SA and carbonyl groups of PHB in the blends were found to be independent of the second component at 3470 cm^{-1} and 1724 cm^{-1}, respectively. The crystallization of PHB was affected by the addition of the SA component both from the melt on cooling and from the glassy state on heating. The temperature and enthalpy of nonisothermal crystallization of PHB in the blends were much lower than those of pure PHB. The crystalline morphology of PHB crystallized from the melt under isothermal conditions varied with SA content. The cold crystallization peaks of PHB in the blends shifted to higher temperatures compared with that of pure PHB. No mechanical study was performed by the authors for their property changes (Zhang et al., 1997) (Table 8-2).

When blends of PHB with cellulose acetate butyrate (CAB) were prepared by solution casting from chloroform solution at different compositions ranging from 20% to 100% PHB, the PHB/CAB blends were found to be miscible in the melt state as evidenced by a single glass transition (T_g) for each composition; a depression in the equilibrium melting point of PHB and a marked reduction in the spherulite growth rate of PHB in the PHB/CAB blends were also detected (Table 8-2). The phase structure of the blend in the solid state as revealed by SAXS (small-angle X-ray scattering) was

TABLE 8-2 Thermal and Mechanical Properties of Typical PHA-based Blends

Sample	Blend Ratio (w/w)	T_g (°C)	T_m (°C)	Young's Modulus (Mpa)	Tensile Strength (Mpa)	Elongation to Break (%)	References
PHB/Starch	70/30	7.1	167	949	19.2	9.4	Godbole et al. (2003)
PHB/SA	40/60	8.6	173		–	–	Zhang et al. (1997)
PHB/PIP-*g*-PVAc	80/20	6	175	711	13.8	13	Yoon et al. (1999)
PHB/BWF	90/10	−20	162	1200	–	–	Fernandes et al. (2004)
a-PHB/P(*d,l*)LA	50/50	23	/	100	–	300	Focarete et al. (2002)
PHB/LMWPLA	50/50	19	145; 167	–	–	–	Koyama and Doi (1997)
PHB/HMWPLA	50/50	5	177	1000	40	80	Park et al. (2004)
UHMWPHB/PLA	70/30	1	177	1600	100	110	Park et al. (2004)
PHBHHx/PLA	60/40	3.7; 65	137; 175	–	–	–	Furukawa et al. (2007)
PHB/P(*d,l*)LA	60/40	0.28; 44.6	175	274	–	27.7	Zhang LL et al. (1996)
PHB/PCL	77/23	−60; 4	60; 168	730	21	9	Kumagai and Doi (1992a)
PHB/PHO	75/25	−35	172	370	6.2	30	Dufresne and Vincendon (2000)
PLA/*a*-PHB	50/50	−1; 66	163	664	12	70	Dacko et al. (2006)
PHB/*a*-PHB	30/70	−1	168	170	3.4	51	Kunze et al. (2006)
PHB/PHBV	25/75	–	152; 163	150	2	7	Sombatmankhong et al. (2006)
PHBV/*a*-PHB	50/50	2	133	240	7	33	Scandola et al. (1997)
PHB/PHBHHx	40/60	0	150	–	18	140	Chen and Wu (2005)
PHB/P3HB4HB	50/50	−10	168	113	3	35	Luo et al. (2007)
PHB/PBA	75/25	–	–	1050	32	7	Ha and Cho (2002)
PHB/EPR	80/20	–	–	147	17	2	Abbate et al. (1991)
PHB/EVA	80/20	–	–	156	17	4	Abbate et al. (1991)
PHB/PEG	80/20	–	166; 152	–	13	40	Parra et al. (2006)

Notes: T_g, glass transition temperature; T_m, melting temperature; –, not determined; SA, starch acetate; PIP-*g*-PVAc, poly(*cis*-1,4-isoprene) grafted with poly(vinyl acetate); BWF, beech wood flour; *a*-PHB, atactic PHB; LMWPLA, low-molecular-weight PLA; HMWPLA, high-molecular-weight PLA; UHMWPHB, ultrahigh-molecular-weight PHB; PBA, poly(1,4-butylene adipate); EPR, ethylene-propylene rubber; EVA, ethylene-vinyl acetate.

characterized by the presence of a homogeneous amorphous phase situated mainly in the interlamellar regions of crystalline PHB and consisting of CAB molecules and noncrystalline PHB chains. Again, there was no study of mechanical property change (El-Shafee et al., 2001).

Pizzoli and co-workers investigated isothermal crystallization from the melt of blends of PHB with two cellulose acetobutyrates (CE1 and CE2) using hot-stage optical microscopy (Pizzoli et al., 1994). Space-filling spherulites were observed at all compositions (50–100% PHB) and crystallization temperatures (50–130°C) were explored. The spherulite radius increases linearly with time, and the radial growth rate (G) depends strongly on the cellulose ester content of the blend. The crystallization rate of the blend containing 50% CE2 is 2.5 orders of magnitude lower than that of pure PHB. The spherulites show banding whose spacing increases with increasing T_c for a given blend, while at constant T_c banding decreases with increasing cellulose ester concentration. In PHB/CEl blends, owing to the ability of CE1 to crystallize from the melt concomitantly with PHB at certain compositions and crystallization temperatures, a very unusual deviation from linearity of the radial growth of PHB spherulites was observed. The rate was seen to increase with time, reflecting the compositional changes that occurred in the melt as a consequence of CE1 crystallization. Apart from the cases where crystallization of CE1 occurred, the morphology of melt-crystallized PHB/CEl and PHB/CE2 blends was rather independent of the identity of the cellulose ester (Pizzoli et al., 1994).

Beech wood flour (BWF) composites were prepared to plasticize PHB. The type of plasticizer [tri(ethylene glycol) bis(2-ethylhexanoate)] (TEGB), poly(ethylene glycol) (PEG200)] and the amounts (5 and 20 wt%) were selected as independent variables in a factorial design. Thermal and mechanical properties of 90 wt% PHB composites were investigated (Table 8-2). Incorporation of PEG200 was found to compromise thermal stability of PHB as demonstrated by the greater decrease in the onset decomposition temperature (T_d) and the drop in its average molecular weight (M_w). The study showed that TEGB/PHB/BWF composites can be optimized to obtain new materials for disposable items (Fernandes et al., 2004).

Lignin fine powder as a new kind of nucleating agent for PHB was studied by Kai et al. (2004). The kinetics of both isothermal and nonisothermal crystallization processes from the melt for both pure PHB and PHB/lignin blend was studied. Lignin shortened the crystallization half-time $t_{1/2}$ for isothermal crystallization. The crystallization of the PHB/lignin blend was more favorable than that of pure PHB from a thermodynamic perspective. At the same time, according to polarized optical microscopy, the rate of spherulite growth from the melt increased with the addition of lignin. Polarized optical microscopy also showed that the spherulites found in PHB with lignin were smaller in size and greater in number than those found in pure PHB. The wide-angle X-ray diffraction (WAXD) indicated that addition of lignin caused no change in the crystal structure and degree of crystallinity. These results indicated that lignin is a good nucleating agent for the crystallization of PHB (Kai et al., 2004).

8.3 PHA BLENDED WITH PLA

The spherulitic structure, growth rates, and melting behavior of blends of bacterially produced PHB and poly(L-lactide) (PLLA) were investigated using polarized light microscopy. Results indicated that low-molecular-weight PLLA ($M_n = 1759$) was miscible in the melt over the whole composition range, whereas a blend of high-molecular-weight PLLA ($M_n = 159{,}400$) with PHB showed biphasic separation (Table 8-2). Two types of spherulite were formed on cooling, related to the crystallization of PHB and PLLA, respectively. In some blends, spherulites of opposite type interpenetrated when the growth fronts met. It is proposed that lamellae belonging to one type of spherulite continued to grow in the interlamellar regions of the other type of spherulite (Blümm and Owen, 1995).

Furukawa and co-workers investigated the miscibility and structure of PHB/PLLA and PHBHHx/PLLA blends using DSC, WAXD, and IR microspectroscopy (Table 8-2). The results are then compared between the two types of blends. They found that both PHB/PLLA and PHBHHx/PLLA blends are immiscible, but the PHBHHx/PLLA blends are somewhat more compatible. WAXD reflection patterns revealed that PHB component can be crystallized in the PHB/PLLA blends with any ratio and that the PHBHHx component can also be crystallized in the PHBHHx/PLLA blends except for the 20/80 blend. The *a* and *b* lattice parameters of each component in the blends are almost constant, suggesting that their crystalline structures are kept intact in the blends. The T_g values for PHBHHx and PLLA components in the PHBHHx/PLLA blends also do not change significantly, as well those for PHB and PLLA component in the PHB/PLLA blends. The observation of the T_c of PLLA in both blend systems suggests that each component in the PHB/PLLA and also in the PHBHHx/PLLA blends forms the mixed semicrystalline structure. These results indicate that the PHB/PLLA blends with decreasing T_c are totally immiscible, while the PHBHHx/PLLA blends with increasing T_c are somewhat compatible. Micro IR spectra from any spots of the 80/20 PHB/PLLA and PHBHHx/PLLA blends show crystalline bands due only to the PHB and PHBHHx components but not for PLLA. On the other hand, although the micro-IR spectra from any spots of the 20/80 PHB/PLLA blend also show the crystalline bands due to PHB, those from some spots of the 20/80 PHBHHx/PLLA blend show only the crystalline bands of the PLLA component. PHBHHx dispersed in a PLLA matrix at this low level does not crystallize (Furukawa et al., 2007) (Table 8-2).

JM Zhang and co-workers investigated the crystallization behaviors of the two components in their immiscible and miscible 50 : 50 blends by real-time infrared (IR) spectroscopy by adjusting the molecular weight of the PLLA component in PHB/PLLA blends (Zhang JM et al., 2006). In the immiscible PHB/PLLA blend, the stepwise crystallization of PHB and PLLA was realized at different crystallization temperatures. PLLA crystallizes first at a higher temperature (120°C). Its crystallization mechanism from the immiscible PHB/PLLA melt was not affected by the presence of the PHB component, while its crystallization rate was substantially depressed. Subsequently, in the presence of crystallized PLLA, the isothermal melt-crystallization of PHB took place at a lower temperature (90°C). It is interesting

to find that there are two growth stages for PHB. At the early stage of the growth period the Avrami exponent is 5.0, which is unusually high, while in the late stage it is 2.5, which is very close to the reported value ($n \approx 2.5$) for the neat PHB system. In contrast to the stepwise crystallization of PHB and PLLA in the immiscible blends, the almost simultaneous crystallization of PHB and PLLA in the miscible 50 : 50 blend was observed at the same crystallization temperature (110°C). Detailed dynamic analysis by IR spectroscopy disclosed that the crystallization of PLLA actually occurs faster than that of PHB even in such apparently simultaneous crystallization. It has been found that in both the immiscible and miscible blends, the crystallization dynamics of PHB are heavily affected by the presence of crystallized PLLA (Zhang JM et al., 2006) (Table 8-2).

Furukawa and co-workers prepared four kinds of PHB/PLLA blends with a PLLA content of 20, 40, 60, and 80 wt% from chloroform solutions. Micro-IR spectra obtained at different positions of a PHB film are all very similar to each other, suggesting that there are no discernible segregated amorphous and crystalline parts on the PHB film at the resolution scale of micro-IR spectroscopy. On the other hand, the micro-IR spectra of two different positions of a PLLA film, where spherulite structures are observed and where they are not observed, are significantly different from each other. PHB and PLLA have characteristic IR marker bands for their crystalline and amorphous components. Therefore, it is possible to explore the structure of each component in the PHB/PLLA blends using micro-IR spectroscopy. The IR spectra of a position of blends except for the 20/80 blend are similar to that of pure PHB. DSC curves of the blend show that the heat of crystallization of PHB varies with the blending ratio of PHB and PLLA. The recrystallization peak is detected for PLLA and the 20/80 blend respectively at 106.5 and 88.2°C. The lowering of recrystallization temperature for the 20/80 blend compared with that of pure PLLA suggests that PHB forms small finely dispersed crystals that may act as nucleation sites of PLLA. The results for the PHB/PLLA blends obtained from IR microspectroscopy indicate that PHB crystallizes in any blends. However, crystalline structures of PHB in the 80/20, 60/40, and 40/60 blends are different from those of the 20/80 blend (Furukawa et al., 2005).

Park and co-workers prepared blends of PLLA with two kinds of PHB having different molecular weights, commercial-grade bacterial PHB (bacterial-PHB) and ultrahigh-molecular-weight PHB (UHMW-PHB), by the solvent-casting method and uniaxially drawn at two drawing temperatures, around the T_g of PHB (2°C) for PHB-rich blends and around the T_g of PLLA (60°C) for PLLA-rich blends. DSC analysis showed that this system was immiscible over the entire composition range (Table 8-2). Mechanical properties of all of the samples were improved in proportion to the draw ratio. Although PLLA domains in bacterial-PHB-rich blends remained almost unstretched during cold drawing, a good interfacial adhesion between two polymers and the reinforcing role of PLLA components led to enhanced mechanical properties proportional to the PLLA content at the same draw ratio (Park et al., 2004).

In contrast, in the case of UHMW-PHB-rich blends, the minor component PLLA was found to be also oriented by cold drawing in ice water due to an increase in the interfacial entanglements caused by the very long chain length of the matrix polymer.

As a result, the mechanical properties were considerably improved with increasing PLLA content compared with the bacterial-PHB system. Scanning electron microscopy observations on the surface and cross-section revealed that a layered structure with uniformly oriented microporous in the interior was obtained by selective removal of PLLA component after simple alkaline treatment (Park et al., 2004).

LL Zhang and co-workers investigated the miscibility, crystallization and morphology of PHB/poly(*d,l*-lactide) (PDLLA) blends. The results indicated that PHB/PDLLA blends prepared by casting a film from a common solvent at room temperature were immiscible over the range of compositions studied, while the melt-blended sample prepared at high temperature showed some evidence of greater miscibility. The crystallization of PHB in the blends was affected by the level of addition of PDLLA. The thermal history caused a depression of the melting point and a decrease in the crystallinity of PHB in the blends. Compared with plain PHB, the blends exhibited some improvement in mechanical properties (Zhang LL et al., 1996).

8.4 PHA BLENDED WITH PCL

Chee and co-workers demonstrated that PEO (poly[ethylene oxide]) is miscible with PHB, whereas poly-ε-caprolactone (PCL) is immiscible (Chee et al., 2002). In their biodegradation, Cara et al. 2003 showed that both pure PCL and PHB samples were degraded with strong erosion of the amorphous zones. In the PCL/PHB 70/30 blend, after only 20 days of incubation, spheres of PCL were bordering with spherulites of PHB, indicating complete degradation. The crystallinity content of homopolymers and blends were investigated at different degradation times: while PCL crystallinity remains constant, both PHB and the blend PHB-phase crystallinity increased. Data from differential scanning calorimetry fit well with those obtained by scanning electron microscopy, gel permeation chromatography, and weight loss analysis (Cara et al., 2003) (Table 8-2).

Two types of mixtures were prepared by solution blending: high molecular weight PHB/PCL and PHB/low-molecular-weight chemically modified PCLs (mPCL). Lovera and co-workers studied the morphology, crystallization, and enzymatic degradation of the blends by exposure to *Aspergillus flavus*. High-molecular-weight PHB/PCL blends were found to be immiscible in the entire composition range. Phenomena such as PCL fractionated crystallization and a decrease in PHB nucleation density were detected. When PHB was blended with mPCLs, the blends were partially miscible; two phases were formed, but the PHB-rich phase exhibited clear signs of miscibility through a depression of both the T_m and the T_g of the PHB component (which was stronger with lower-molecular-weight mPCL), and an increase in the growth rate of PHB spherulites in the blends as compared with neat PHB or the PHB component in the PHB/PCL blends. The biodegradation by exposure to *A. flavus* showed that the blends are synergistically attacked in comparison with the homopolymers. Two factors may influence the improved degradation rate of the blends: the dispersion of the components and their crystallinity, which was reduced

in view of the fractionated crystallization and transfer of impurities. In the case of the PHB/mPCL blends, the increased miscibility between the components caused a reduction in the degradation rate (Lovera et al., 2007).

8.5 BLENDING OF DIFFERENT PHAs

Dufresne and Vincendon (2000) prepared blends of PHB with poly(3-hydroxyoctanoate) (PHO) by co-dissolving the two polyesters in chloroform and casting the mixture. It has been observed that PHB shows no miscibility at all with PHO, resulting in two-phase systems in which the nature of the continuous phase is composition-dependent. The morphology of the blend strongly influences the mechanical behavior. The mechanical properties of these materials have been predicted from a model involving the percolation concept. It takes both linear and nonlinear mechanical behaviors into account and allows for the effect of the lack of adhesion between material domains and/or breakage of one of the components (Dufresne and Vincendon, 2000).

Scandola and co-workers blended synthetic atactic PHB (*a*-PHB) with a natural bacterial PHBV containing 10 mol% of 3HV using a simple casting procedure (Table 8-2). In the range of compositions explored (10–50% *a*-PHB), blends of PHBV and synthetic atactic *a*-PHB were miscible in the melt and solidified with spherulitic morphology. The degree of crystallinity decreased with increasing content of *a*-PHB in the film samples, and the elongation at break for a sample containing 50% of *a*-PHB was 30-fold that of pure PHBV. Degradation experiments using both hydrolytic (pH 7.4, 70°C) and enzymatic PHB depolymerase A from *Pseudomonas lemoignei* or Tris-HCl buffer (pH 8, 37°C) were performed for both polymers and polymer blends. The rate of enzymatic degradation of the blends was higher than that of PHBV and increased with *a*-PHB content in the blends studied, whereas pure *a*-PHB did not biodegrade under these conditions. 3-Hydroxybutyric acid (3HB) and its dimer were identified by HPLC as biodegradation products of both pure PHBV and its blends with *a*-PHB. Higher oligomers up to heptamer were detected as degradation products of the blends by APCI-MS and ESI-MS (Scandola et al., 1997).

Saito and co-workers showed that the PHB/PHBV (9% HV) blends exhibited almost perfect cocrystallization, the PHB/PHBV (15% HV) blends form PHB-rich crystalline phase, and the PHB/PHB (21% HV) blends showed phase segregation and formation of the crystalline phases of component polymers as well as the cocrystalline phase. These results indicate that the degree of phase segregation changes depending on the HV content of PHBV. As the HV content increases, phase segregation proceeds to higher degree before cocrystallization and, as a result, the copolymer content in the cocrystalline phase decreases and/or the crystalline phases of the component polymers are formed. The phase structure of the blends is determined by the competition between cocrystallization and phase segregation. The necessary conditions for cocrystallization are supposed to be miscibility in the melt state, similarity of the crystalline structures, similarity of the crystallization rates of the component polymers, and large crystallization rates. The miscibility prevents phase segregation.

The similarity of the crystalline structure lowers the free energy of cocrystallization. The similarity of the crystallization rates allows the simultaneous crystallization of two components. The high crystallization rate does not give sufficient time for phase segregation. It has been reported that the crystalline lattice of PHBV containing 40% or less HV unit is the same as that of PHB. The fact that PHB and PHBV with high HV content are immiscible indicates that the extent of miscibility between PHB and PHBV gradually decreases with the increase of HV content of PHBV. The fact that the crystallization rate of PHBV gradually decreases with the increase of HV content shows that the difference in the crystallization rate of component polymers gradually increases with the increase of HV content of PHBV. Both of these factors promote phase segregation with the increase of the HV content of PHBV for PHB/PHBV blends. Therefore, as the HV content of PHBV for PHB/PHBV blends increases, the PHBV content in the cocrystalline phase gradually decreases and the crystalline phases of the individual component polymers are formed (Saito et al., 2001).

The hydrolytic degradation of PHBV and PHO blends with low- and high-molecular-weight additives was examined. DSC and atomic force microscopy (AFM) results revealed that hydrolyzable PLA and hydrophilic PEG, selected as additives that might accelerate hydrolytic degradation, were immiscible with PHBV or PHO over the range of compositions studied. The results show that the presence of a second component, whatever its chemical nature, is sufficient to perturb the crystallization behavior of highly crystalline PHBV, and increase hydrolytic degradation. In contrast, the degradation of PHO was unaffected by blending with PLA or PEG. PHO degradation is a very slow process, requiring several months of incubation. However, the introduction of polar carboxylic groups in side-chains led to an increase in the degradation rate. Carboxylic groups promote water penetration into the polymer (Renard et al., 2004) (Table 8-2).

8.6 PHA BLENDED WITH OTHER POLYMERS

De Lima and Felisberti showed that PHB/PEP (poly[epichlorohydrin]) and PHB/ECO (poly[epichlorohydrin-co-ethylene oxide]) blends are immiscible. The apparent melting temperature (T_m) of PHB in the blends decreases slightly with increasing elastomeric content and the melting point depression cannot be associated with miscibility, because the blends are immiscible. Thus, T_m of the blends are affected by morphological effects. There is an influence of PEP and ECO on the crystallization that occurs upon cooling of PHB, even when the blends are immiscible due to an expressive decrease of the intensity of the peak at crystallization, that is completed during the second heating. The degree of crystallinity of blends with PEP was found to decrease with an increase in PEP content. PHB/ECO blends exhibit degrees of crystallinity that can be considered nearly independent of the ECO content. Study of the morphology of blends showed that the presence of elastomer influences the ratio of the growth rate and the nucleation rate. The elastomer component, probably resides in the intraspherulitic zones (de Lima and Felisberti, 2006).

Xing and co-workers made a systematic study of the miscibility, crystallization, and morphology of PHB/PVPh [poly(*p*-vinylphenol)] blends (Xing et al., 1997). The single glass transition temperatures of the blends suggest that PHB and PVPh will form miscible blends in the whole composition range in melt. After quenching, the melting enthalpy of PHB in the blend is substantially lowered and approaches zero at about 40% PVPh content, which is due to the high glass transition temperature of the blend. The equilibrium melting point of PHB in the blends, which was obtained from DSC results using the Hoffman–Weeks equation, decreases with the increase in PVPh content. The large negative values of the interaction parameter determined from the equilibrium melting point depression support the miscibility and strong hydrogen-bonding interactions between the components. They found that the rate of isothermal crystallization of PHB is strongly affected by blending it with PVPh. The rate of spherulite growth decreases with the increase in PVPh content. Isothermally crystallized blends of PHB with PVPh were examined by WAXD and SAXS. The long period increases with the addition of amorphous PVPh, which is a strong indication of interlamellar segregation (Xing et al., 1997).

Qiu and co-workers prepared four blends of PHB and poly(butylene succinate) (PBS), both biodegradable semicrystalline polyesters, with the ratio of PHB/PBS ranging from 80/20 to 20/80 by co-dissolving the two polyesters in *N*,*N*-dimethylformamide and casting the mixture. Results indicated that PHB showed some limited miscibility with PBS for PHB/PBS 20/80 blend as evidenced by the small change in the glass transition temperature and the depression of the equilibrium melting point temperature of the high-melting-point component PHB. However, PHB showed immiscibility with PBS for the other three blends as shown by the existence of unchanged composition-independent glass transition temperature and the biphasic melt. During the nonisothermal crystallization of PHB/PBS blends, two crystallization peak temperatures were found for PHB/PBS 40/60 and 60/40 blends, corresponding to the crystallization of PHB and PBS, respectively, whereas only one crystallization peak temperature was observed for PHB/PBS 80/20 and 20/80 blends. However, it was found that after the nonisothermal crystallization the crystals of PHB and PBS actually co-existed in PHB/PBS 80/20 and 20/80 blends from the two melting endotherms observed in the subsequent DSC melting traces, corresponding to the melting of PHB and PBS crystals, respectively. The subsequent melting behavior was also studied after nonisothermal crystallization. In some cases, double melting behavior was found for both PHB and PBS, which was influenced by the cooling rates used and the blend composition (Qiu et al., 2003).

Parra and co-workers investigated the thermal properties, tensile properties, water vapor transmission rate, enzymatic biodegradation and mass retention of blends of PHB with PEG (PHB/PEG), in proportions of 100/0, 98/2, 95/5, 90/10, 80/20, and 60/40 wt%, respectively. They found that the addition of plasticizer did not alter the thermal stability of the blends, although an increase in the PEG content reduced the tensile strength and increased the elongation at break of pure PHB (Parra et al., 2006) (Table 8-2).

8.7 PHA COMPOSITES

It has been demonstrated that the incorporation of a small amount of α-cyclodextrin can greatly enhance the nucleation and crystallization of PHB. This natural and environmentally safe compound, may thus be used as a nucleation agent for biodegradable polyester PHB (He and Inoue, 2003).

The di-*n*-butyl phthalate (DBP) diluent is miscible at molecular level with the natural polyester PHB. In PHB/DBP mixtures both the glass transition and melting temperatures decrease with increasing diluent content, the shift of T_g being more pronounced than that of T_m. The whole crystallization window moves to lower temperatures and broadens, as reflected by the changes of the cold crystallization process in dynamic DSC scans and by the shifts of the isothermal spherulite growth rate curves. It is interesting to note that the maximum growth rate (G_{max}) does not change in the range of diluent contents explored and that all isothermal crystallization data fall on the same master curve when the crystallization temperatures are normalized to account for the T_g and T_m changes with composition. The constancy of G_{max} indicates that in the polymer–diluent mixtures investigated, opposite "dilution" and "chain mobility" effects that should respectively decrease and increase the crystal growth rates tend to compensate (Pizzoli et al., 2002).

Ceccorulli and co-workers found blends obtained by melt compounding of PHB with CAB are miscible over the whole composition range. In the range of PHB contents from 0% to 50% the blend glass transition temperature (T_g) depends strongly on composition, while a much less substantial dependence is found when the amount of PHB exceeds 50%. In the former composition range, in addition to the strongly composition-dependent T_g, another relaxation associated with mobilization of the low-T_g component is observed at a lower temperature (Ceccorulli et al., 1993).

The DBP is miscible in all proportions with both CAB and PHB. Analogously to the polymeric CAB/PHB blends, the two polymer/diluent systems investigated (CAB/DBP and PHB/DBP) show a dual dependence of T_g on composition. In binary mixtures such behavior appears to be independent of the macromolecular or low-molecular-weight nature of the low-T_g component. Addition of a fixed amount of DBP plasticizer to CAB/PHB blends with varying composition (PHB content from 0% to 100%) causes a significant decrease of T_g of the binary polymer blends; the T_g depression is larger the higher the amount of DBP in the ternary blend. Concomitant with the expected "plasticizing" effect on T_g, the presence of DBP also induces a decrease in the characteristic temperature of the additional low-temperature transition observed in CAB/PHB blends. In the ternary blends, the temperature of such a transition is a function of DBP content only, being independent of the relative amount of the two polymers (CAB and PHB) (Ceccorulli et al., 1993).

In conclusion, the many efforts that have been made to improve the properties of PHA, including blending and composite preparations, have achieved various degrees of success. In the future, blends or composite preparation should be tailor made to suite a particular application. With increasing costs of petrochemicals, more and more effort is being directed to the development of useful biobased materials for various application for PHA; some of these effects will be rewarded sooner or later.

REFERENCES

Abbate M, Martuscelli E, Ragosto G, Scarinzi G. 1991. Tensile properties and impact behaviour of poly(D(−)3-hydroxybutyrate)/rubber blends. *J Mater Sci* 26:1119–1125.

Abe H, Matsubara I, Doi Y. 1995. Physical properties and enzymic degradability of polymer blends of bacterial poly[(*R*)-3-hydroxybutyrate] and poly[(*R,S*)-3-hydroxybutyrate] stereoisomers. *Macromolecules* 28:844–853.

Anderson AJ, Dawes EA. 1990. Occurrence, metabolism, metabolic role and industrial uses of bacterial polyhydroxyalkanoates. *Microbiol Rev* 45:450–472.

Avella M, Martuscelli E. 1988. Poly-D-(−)(3-hydroxybutyrate)/poly(ethylene oxide) blends: phase diagram, thermal and crystallization behavior. *Polymer* 29:1731–1737.

Azuma Y, Yoshie N, Sakurai M, Inoue Y, Chu JR. 1992. Thermal behaviour and miscibility of poly(3-hydroxybutyrate)/poly(vinyl alcohol) blends. *Polymer* 33:4763–4767.

Blümm E, Owen AJ. 1995. Miscibility, crystallization and melting of poly(3-hydroxybutyrate)/poly(L-lactide) blends. *Polymer* 36:4077–4081.

Byrom D. 1992. Production of poly-β-hydroxybutyrate and poly-β-hydroxyvalerate copolymers. *FEMS Microbiol Rev* 103:247–250.

Cara FL, Immirzi BE, Mazzella A, Portofino S, Orsello G, De Prisco PP. 2003. Biodegradation of poly-ε–caprolactone/poly-β-hydroxybutyrate blend. *Polym Degrad Stab* 79:37–43.

Ceccorulli G, Pizzoli M, Scandola M. 1993. Effect of a low molecular weight plasticizer on the thermal and viscoelastic properties of miscible blends of bacterial poly(3-hydroxybutyrate) with cellulose acetate butyrate. *Macromolecules* 26:6722–6726.

Chee MJK, Ismail J, Kummerlöwe C, Kammer HW. 2002. Study on miscibility of PEO and PCL in blends with PHB by solution viscometry. *Polymer* 43:1235–1239.

Chen GQ. 2003. Production and application of microbial polyhydroxyalkanoates. In: Chiellini E, Solaro R, editors. *Biodegradable Polymers and Plastics* (Proceedings of the 7th World Conference on Biodegradable Polymers & Plastics). Kluwer Academic/Plenum. p. 155–166.

Chen GQ, Wu Q. 2005. Polyhydroxyalkanoates as tissue engineering materials. *Biomaterials* 26:6565–6578.

Chen GQ, Koenig KH. Lafferty RM. 1991. Production of poly-D(−)-3-hydroxybutyrate and poly-D(−)-3-hydroxyvalerate by strains of *Alcaligenes latus*. *Antonie van Leeuwenhoek* 60:61–66.

Chen GQ, Wu Q, Zhao K, Yu HP, Chan A. 2000. Chiral Biopolyesters-Polyhydroxyalkanoates Synthesized by Microorganisms. Chinese. *J Polym Sci* 18:389–396.

Chen GQ, Zhang G, Park SJ, Lee SY. 2001. Industrial production of poly(hydroxybutyrate-co-hydroxyhexanoate). *Appl Microbiol Biotechnol* 57:50–55.

Dacko P, Kowalczuk M, Janeczek H, Sobota M. 2006. Physical properties of the biodegradable polymer compositions containing natural polyesters and their synthetic analogues. *Macromol Symp* 239:209–216.

de Lima JA, Felisberti MI. 2006. Poly(hydroxybutyrate) and epichlorohydrin elastomers blends: Phase behavior and morphology. *Eur Polym J* 42:602–614.

Doi Y, Kitamura S, Abe H. 1995. Microbial synthesis and characterization of poly(3-hydroxybutyrate-co-3-hydroxyhexanoate). *Macromolecules* 28:4822–4828.

Dubini PE, Beltrame PL, Canetti M, Seves A, Marcandalli B, Martuscelli E. 1993. Crystallization and thermal behaviour of poly-D(−)3-hydroxybutyrate)/poly(epichlorohydrin) blends. *Polymer* 34:996–1001.

Dufresne A, Vincendon M. 2000. Poly(3-hydroxybutyrate) and poly(3-hydroxyoctanoate) blends: morphology and mechanical behavior. *Macromolecules* 33:2998–3008.

El-Shafee E, Saad GR, Fahmy SM. 2001. Miscibility, crystallization and phase structure of poly(3-hydroxybutyrate)/cellulose acetate butyrate blends. *Eur Polym J* 37:2091–2104.

Fernandes EG, Pietrini M, Chiellini E. 2004. Bio-based polymeric composites comprising wood flour as filler. *Biomacromolecules* 5:1200–1205.

Focarete ML, Scandola M, Dobrzynski P, Kowalczuk M. 2002. Miscibility and mechanical properties of blends of (L)-lactide copolymers with atactic poly(3-hydroxybutyrate). *Macromolecules* 35:8472–8477.

Furukawa T, Sato H, Murakami R, et al. 2005. Structure, dispersibility, and crystallinity of poly(hydroxybutyrate)/poly(L-lactic acid) blends studied by FT-IR microspectroscopy and differential scanning calorimetry. *Macromolecules* 38:6445–6454.

Furukawa T, Sato H, Murakami R, et al. 2007. Comparison of miscibility and structure of poly(3-hydroxybutyrate-co-3-hydroxyhexanoate)/poly(L-lactic acid) blends with those of poly(3-hydroxybutyrate)/poly(L-lactic acid) blends studied by wide angle X-ray diffraction, differential scanning calorimetry, and FTIR microspectroscopy. *Polymer* 48: 1749–1755.

Gassner F, Owen AJ. 1996. Some properties of poly(3-hydroxybutyrate)-poly(3-hydroxyvalerate) blends. *Polym Int* 39:215–219.

Godbole SS, Gote M, Latkar T, Chakrabarti S. 2003. Preparation and characterization of biodegradable poly-3-hydroxybutyrate–starch blend films. *Bioresource Technol.* 86:33–37.

Greco P, Martuscelli E. 1989. Crystallization and thermal behaviors of poly(D-3-hydroxybutyrate)-based blends. *Polymer* 30:1475–1483.

Ha CS, Cho WJ. 2002. Miscibility, properties and biodegradability of microbial polyester containing blends. *Prog Polym Sci* 27:759–809.

He Y, Inoue Y. 2003. α-Cyclodextrin enhanced crystallization of poly(3-hydroxybutyrate). *Biomacromolecules* 4:1865–1867.

Hrabak O. 1992. Industrial production of poly-β-hydroxybutyrate. *FEMS Microbiol Rev* 103: 251–256.

Kai WH, He Y, Asakawa N, Inoue Y. 2004. Effect of lignin particles as a nucleating agent on crystallization of poly(3-hydroxybutyrate). *J Appl Polym Sci* 94:2466–2474.

Kim MN, Lee AR, Lee KH, Chin IJ, Yoon JS. 1999. Biodegradability of poly(3-hydroxybutyrate) blended with poly(ethylene-co-vinyl acetate) or poly(ethylene oxide). *Eur Polym J* 35:1153–1158.

Koyama N, Doi Y. 1997. Miscibility of binary blends of poly[(*R*)-3-hydroxybutyric acid] and poly[(*S*)-lactic acid]. *Polymer* 38:1589–1593.

Kumagai Y, Doi Y. 1992a. Enzymatic degradation and morphologies of binary blends of microbial poly(3-hydroxy butyrate) with poly(ε-caprolactone), poly(1,4-butylene adipate and poly(vinyl acetate). *Polym Degrad Stab* 36:241–248.

Kumagai Y, Doi Y. 1992b. Enzymatic degradation of binary blends of microbial poly(3-hydroxybutyrate) with enzymatically active polymers. *Polym Degrad Stab* 37:253–256.

Kumagai Y, Doi Y. 1993. Synthesis of a block copolymer of poly(3-hydroxybutyrate) and poly(ethylene glycol) and its application to biodegradable polymer blends. *J Environ Polym Degrad* 1:81–87.

Kunze C, Bernd HE, Androsch R, et al. 2006. In vitro and in vivo studies on blends of isotactic and atactic poly(3-hydroxybutyrate) for development of a dura substitute material. *Biomaterials* 27:192–201.

Lotti N, Pizzoli M, Ceccorulli G, Scandola M. 1993. Binary blends of microbial poly(3-hydroxybutyrate) with polymethacrylates. *Polymer* 34:4935–4940.

Lovera D, Marquez L, Balsamo V, Taddei A, Castelli C, Müller AJ. 2007. Crystallization, morphology, and enzymatic degradation of polyhydroxybutyrate/polycaprolactone (PHB/PCL) blends. *Macromo. Chem Phys* 208:924–937.

Luo RC, Xu KT, Chen GQ. 2007. Miscibility, crystallization, mechanical properties and thermal stability of blends of poly(3-hydroxybutyrate) and poly(3-hydroxybutyrate-co-4-hydroxybutyrate). *J Appl Polym Sci* 105:3402–3408.

Organ SJ, Barham PJ. 1993. Phase separation in a blend of poly(hydroxybutyrate) with poly(hydroxybutyrate-co-hydroxyvalerate). *Polymer* 34:459–467.

Park JW, Doi Y, Iwata T. 2004. Uniaxial drawing and mechanical properties of poly[(*R*)-3-hydroxybutyrate]/poly(L-lactic acid) blends. *Biomacromolecules* 5:1557–1566.

Parra DF, Fusaro J, Gaboardi F, Rosa DS. 2006. Influence of poly (ethylene glycol) on the thermal, mechanical, morphological, physical-chemical and biodegradation properties of poly(3-hydroxybutyrate). *Polym Degrad Stab* 91:1954–1959.

Pearce RP, Marchessault RH. 1994. Melting and crystallization in bacterial poly(β-hydroxyvalerate), PHV, and blends with poly(β-hydroxybutyrate-co-hydroxyvalerate). *Macromolecules* 27:3869–3874.

Pizzoli M, Scandola M, Ceccorulli G. 1994. Crystallization kinetics and morphology of poly(3-hydroxybutyrate)/cellulose ester blends. *Macromolecules* 27:4755–4761.

Pizzoli M, Scandola M, Ceccorulli C. 2002. Crystallization and melting of isotactic poly(3-hydroxy butyrate) in the presence of a low molecular weight diluent. *Macromolecules* 35:3937–3941.

Qiu Z, Ikehara T, Nishi T. 2003. Poly(hydroxybutyrate)/poly(butylene succinate) blends: miscibility and nonisothermal crystallization. *Polymer* 44:2503–2508.

Renard E, Walls M, Guerin P, Langlois V. 2004. Hydrolytic degradation of blends of polyhydroxyalkanoates and functionalized polyhydroxyalkanoates. *Polym Degrad Stab* 85: 779–787.

Sadocco P, Canetti M, Seves A, Marcandalli B, Martuscelli E. 1993. Small-angle X-ray scattering study of the phase structure of poly(D-(−)-3-hydroxybutyrate) and atactic poly(epichlorohydrin) blends. *Polymer* 34:3368–3375.

Saito M, Inoue Y, Yoshie N. 2001. Cocrystallization and phase segregation of blends of poly(3-hydroxybutyrate) and poly(3-hydroxybutyrate-co-3-hydroxyvalerate). *Polymer* 42: 5573–5580.

Scandola M, Ceccorulli G, Pizzoli M. 1992. Miscibility of bacterial poly(3-hydroxybutyrate) with cellulose esters. *Macromolecules* 25:6441–6446.

Scandola M, Focarete ML, Grazyna AG, et al. 1997. Polymer blends of natural poly(3-hydroxybutyrate-*co*-3-hydroxyvalerate) and a synthetic atactic poly(3-hydroxybutyrate). Characterization and biodegradation studies. *Macromolecules* 30:2568–2574.

Sombatmankhong K, Suwantong O, Waleeforncheepsawat S, Supaphol P. 2006. Electrospun fiber mats of poly(3-hydroxybutyrate), poly(3-hydroxybutyrate-co-3-hydroxyvalerate), and their blends. *J Polym Sci Part B Polym Phys* 4:2923–2933.

Verhoogt H, Ramsay BA, Favis BD. 1994. Polymer blends containing poly(3-hydroxyalkanoate)s. *Polymer* 35:5155–5169.

Weusthuis RH, Kessler B, Dielissen MPM, Witholt B, Eggink G. 2002. Fermentative production of medium-chain-length poly(3-hydroxyalkanoate). In: Doi Y, Steinbüchel A, editors. *Biopolymers (Polyesters I)*. New York: Wiley–VCH. p. 291–316.

Xing P, Dong L, An Y, Feng Z, Avella M, Martuscelli E. 1997. Miscibility and crystallization of poly(α-hydroxybutyrate) and poly(*p*-vinylphenol) blends. *Macromolecules* 30: 2726–2733.

Yoon JS, Choi CS, Maing SJ, Choi HJ, Lee HS, Choi SJ. 1993. Miscibility of poly-D(−)(3-hydroxybutyrate) in poly(ethylene oxide) and poly(methyl methacrylate). *Eur Polym J* 29:1359–1364.

Yoon JS, Chang MC, Kim MN, Kang EJ, Kim C, Chin IJ. 1996. Compatibility and fungal degradation of poly[(*R*)-3-hydroxybutyrate]/aliphatic copolyester blend. *J Polym Sci Part B Polym Phys* 34:2543–2551.

Yoon JS, Lee WS, Jin HJ, Chin IJ, Kim MN, Go JH. 1999. Toughening of poly(3-hydroxybutyrate) with poly(*cis*-1,4-isoprene). *Eur Polym J* 35:781–788.

Zhang JM, Sato H, Furukawa T, Tsuji H, Noda I, Ozaki Y. 2006. Crystallization behaviors of poly(3-hydroxybutyrate) and poly(L-lactic acid) in their immiscible and miscible blends. *J Phys Chem B* 110:24463–24471.

Zhang LL, Xiong CD, Deng XM. 1996. Miscibility, crystallization and morphology of poly(*p*-hydroxybutyrate)/poly(D,L-lactide) blends. *Polymer* 37:235–241.

Zhang LL, Deng XM, Zhao SJ, Huang ZT. 1997. Biodegradable polymer blends of poly(3-hydroxybutyrate) and starch acetate. *Polym Int* 44:104–110.